Proceedings of
11th European Conference on Turbomachinery Fluid dynamics & Thermodynamics
ETC11, March 23-27, 2015, Madrid, Spain

Invited Lecture of ETC11

11th EUROPEAN CONFERENCE
TURBOMACHINERY FLUID DYNAMICS AND THERMODYNAMICS

European Turbomachinery Conference

Madrid, Spain
March 23-27, 2015

RECENT ADVANCES IN THE ANALYSIS AND DESIGN OF MARINE PROPULSORS

by Professor Spyros A. Kinnas
Ocean Engineering Group (OEG)
Department of Civil, Architectural and Environmental Engineering
The University of Texas at Austin

Some marine propulsor configurations:
(other than common propellers)

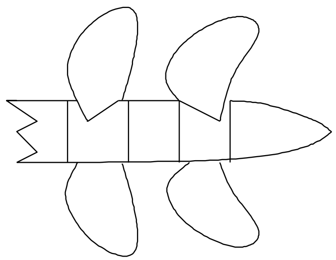

contra-rotating

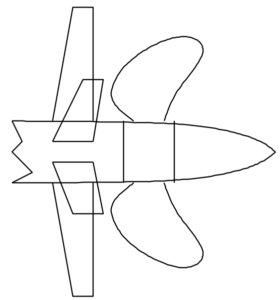

stator/rotor

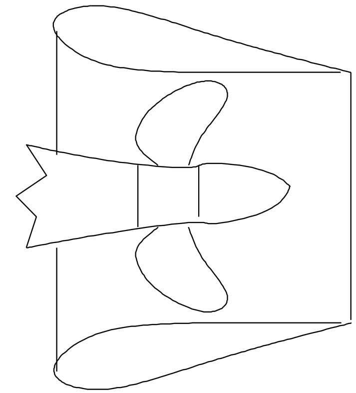

ducted **(or thrusters)**

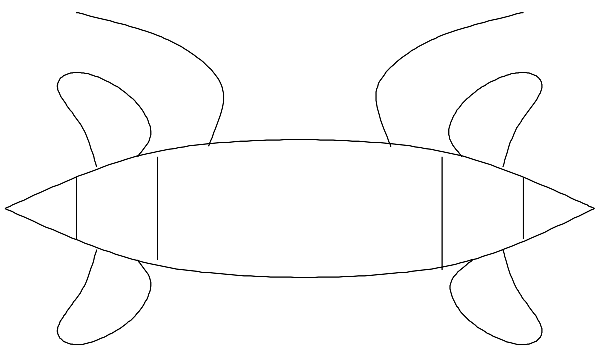

podded

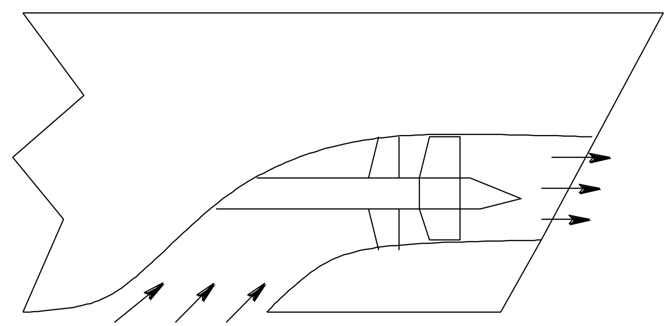

water-jet

The "Holy Super-Grail" of Naval Architecture! Simulate the motion (6 DOF) of a ship in waves (and wind!) including its interaction with propeller.

The two "wakes"…

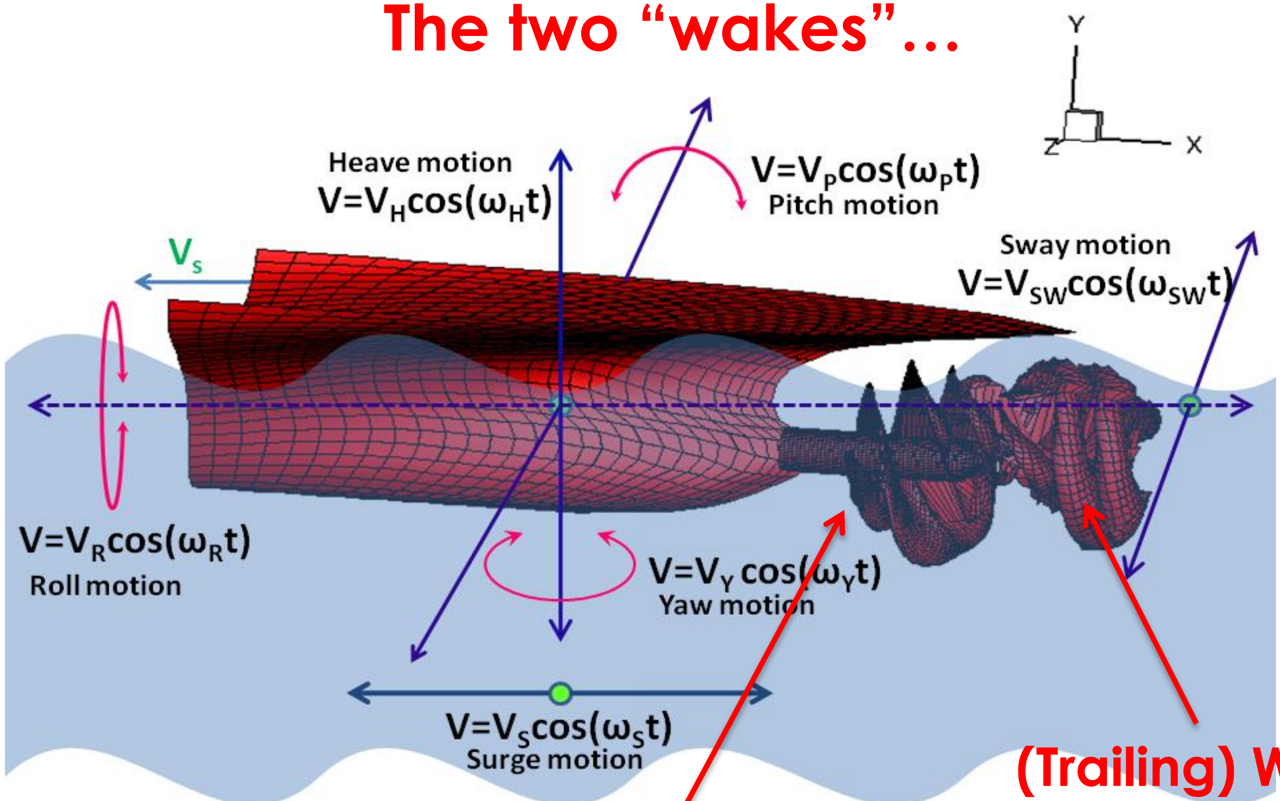

(Trailing) Wake:
Means Trailing vorticity in the Wake of the propeller

(Inflow) Wake:
Means Inflow to Propeller due to Ship's Wake

Analysis of single (open) propellers

Cavitation (of various types) is quite often present

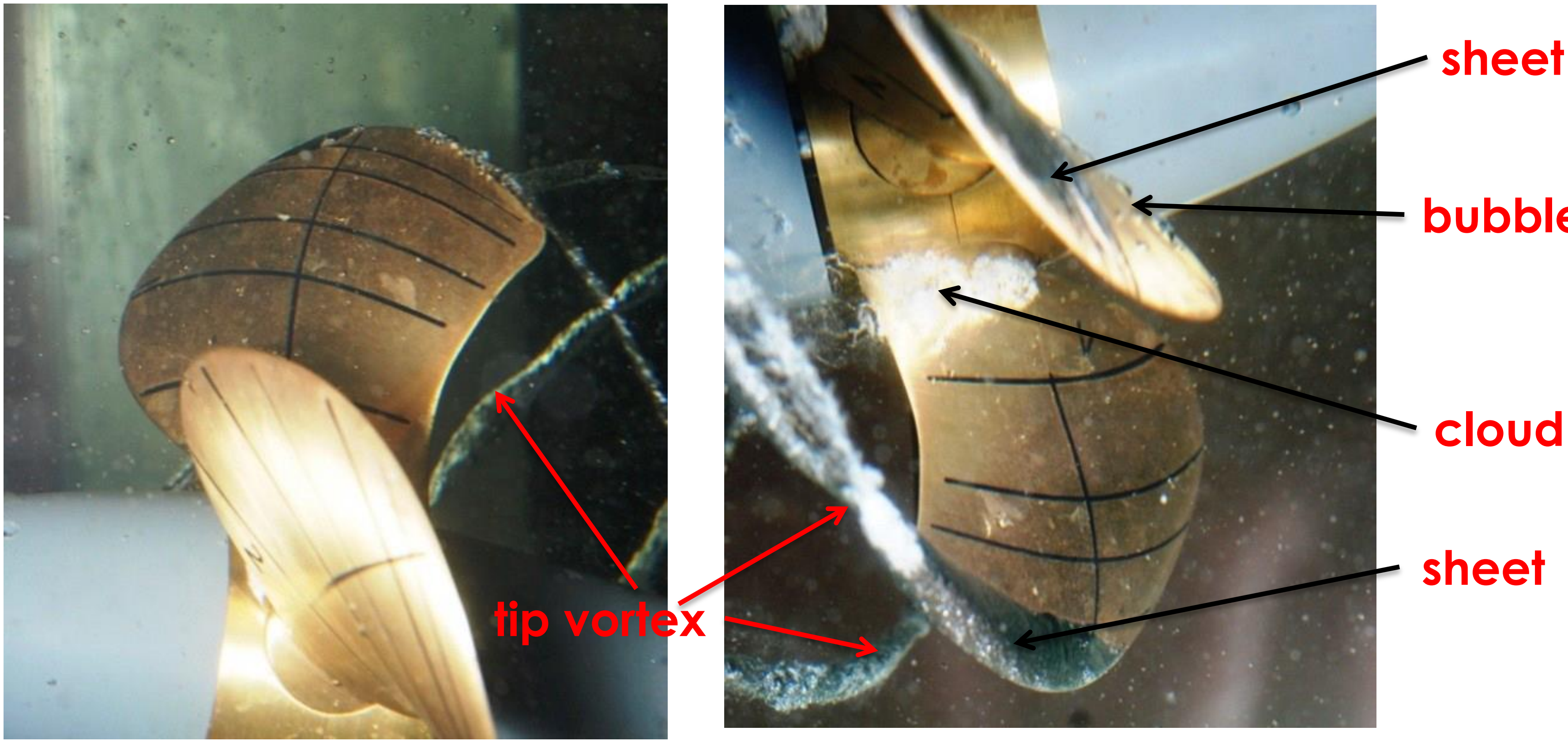

Experiments performed at *Potsdam Model Basin (Germany) – to be used for validation of computational methods at Workshop at* ***SMP'15*** *(4th Symposium on Marine Propulsors),* ***May 31-June 4, 2015, UT Austin***

Our approach/models for single propellers subject to non-uniform/non-axisymmetric inflow, with the presence of sheet and/or developed tip vortex cavitation

Definition of blade geometry

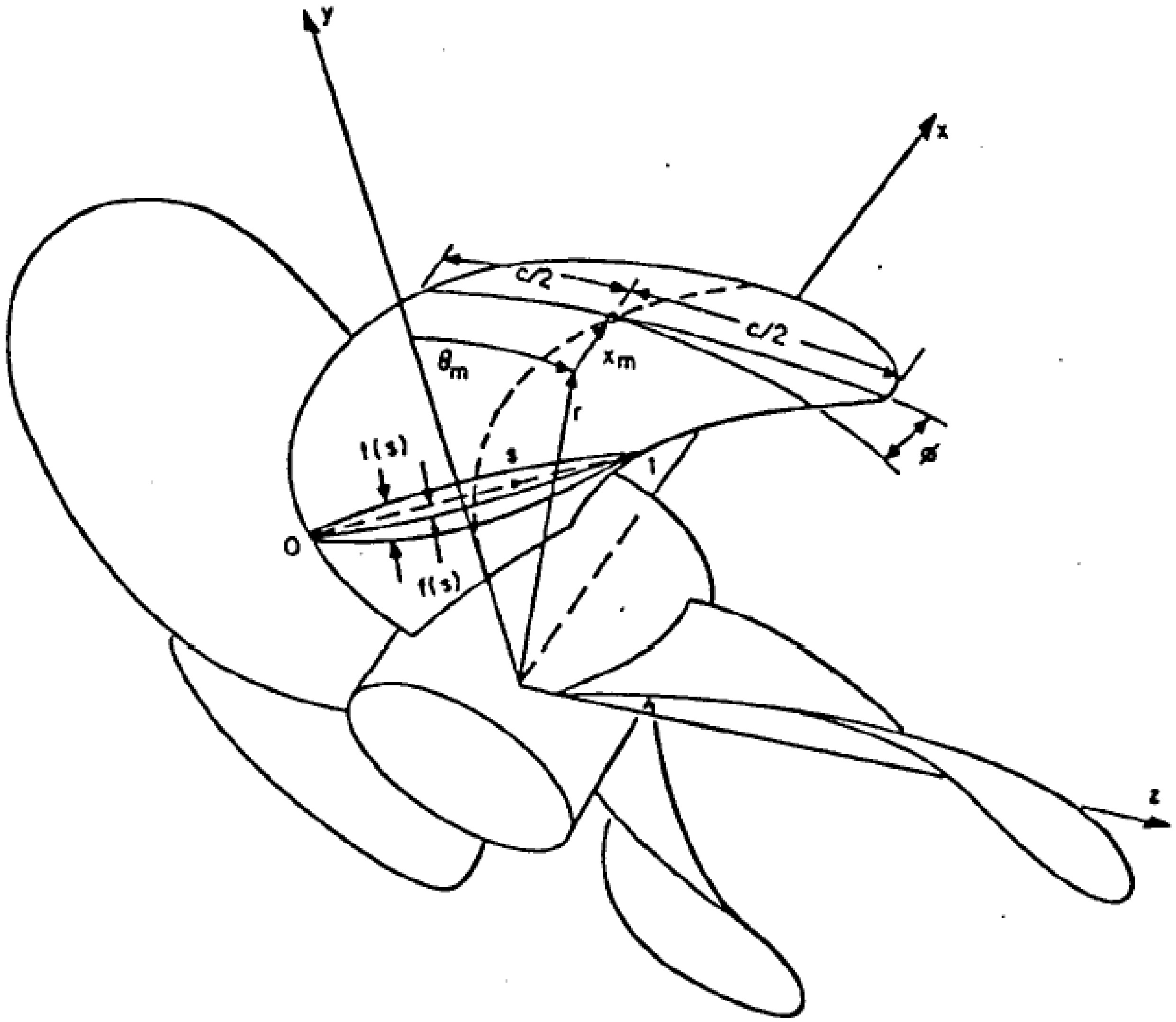

Nomenclature:

C_p	Pressure Coefficient, $C_p = (P - P_o)/(\rho n^2 D^2)$
C_T	Thrust Coefficient for stator, $C_T = T/\frac{1}{2}\rho V_s^2 \pi R^2$
C_Q	Torque Coefficient for stator, $C_Q = Q/\frac{1}{2}\rho V_s^2 \pi R^3$
D	Diameter of Propeller
F_r	Froude Number $F_r = n^2 D/g$
g	Gravitational Acceleration
Γ	Circulation
G	Non-Dimensional Circulation, $G = \Gamma \times 10^2/(2\pi R V_R)$
J_s	Advance Ratio, $J_s = V_s/nD$
K_T	Thrust Coefficient for propeller, $K_T = T/\rho n^2 D^4$
K_Q	Torque Coefficient for propeller, $K_Q = Q/\rho n^2 D^5$
n	Propeller Rotational Frequency (rev/s)
P	Pressure
P_o	Pressure Far Upstream at the propeller axis
P_v	Vapor Pressure of Water
$\vec{q}_{in}$	Local Inflow Velocity
Q	Torque
R or R_p	Radius of Propeller
T	Thrust
V_s	Ship Speed
V_R	Reference Velocity, $V_R = \sqrt{V_s^{\,2} + (0.7n\pi D)^2}$
ρ	Fluid Density
σ_n	Cavitation Number Based on n, $\sigma_n = (P - P_v)/(\frac{\rho}{2} n^2 D^2)$
σ_v	Cavitation Number Based on V_s, $\sigma_v = (P - P_v)/(\frac{\rho}{2} V_s^{\,2})$

Vortex (and Source)-Lattice Methods (VLM) (also called Quasi-Continuous Method-QCM)

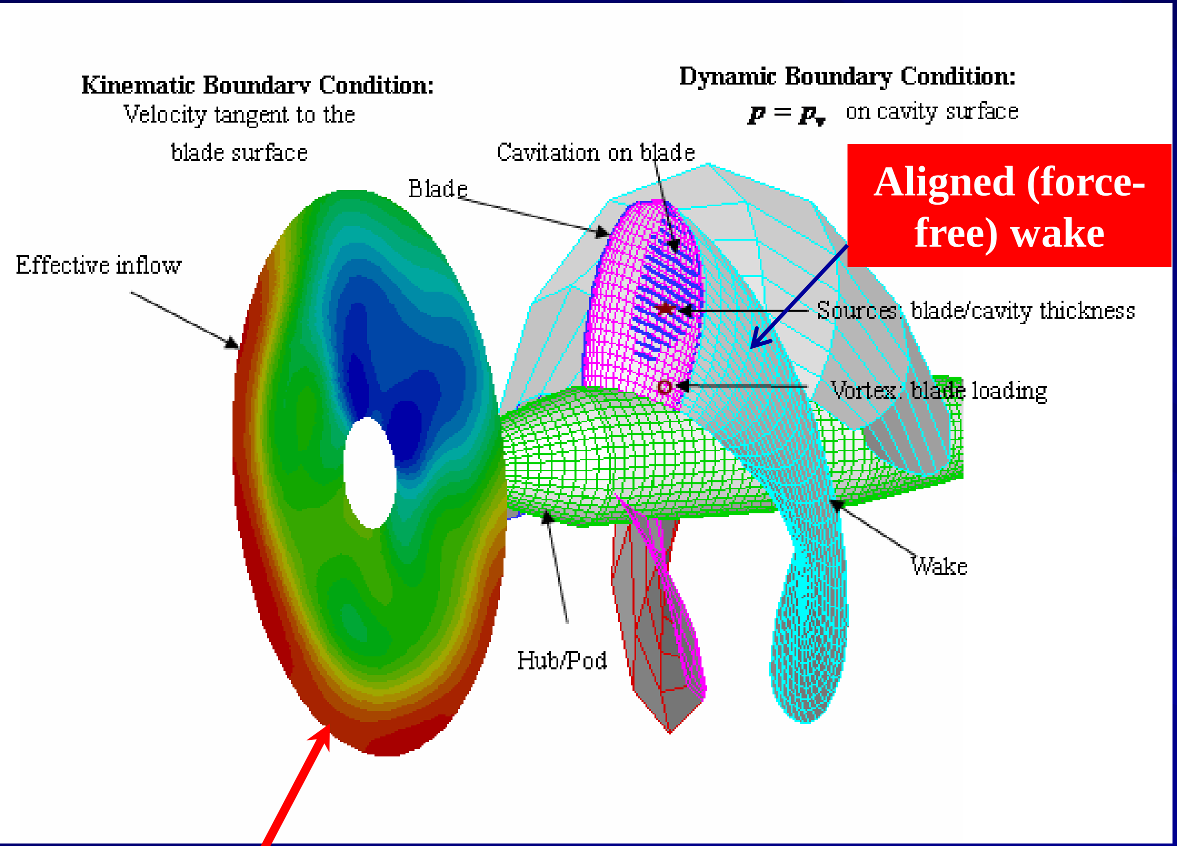

- Lattice is placed on **mean** camber & wake surface
- **Fully unsteady** (NOT quasi-steady)
- Solve for bound vortex and cavity source **unsteady strengths**
- Determine **unsteady** pressure distributions and **sheet cavity** patterns on blade

Non-axisymmetric (<u>effective wake</u>) inflow

- **PUF-3A (code name): developed at MIT**
- **MPUF-3A : further developed at UT**

Boundary Element (Panel) Methods (BEM)

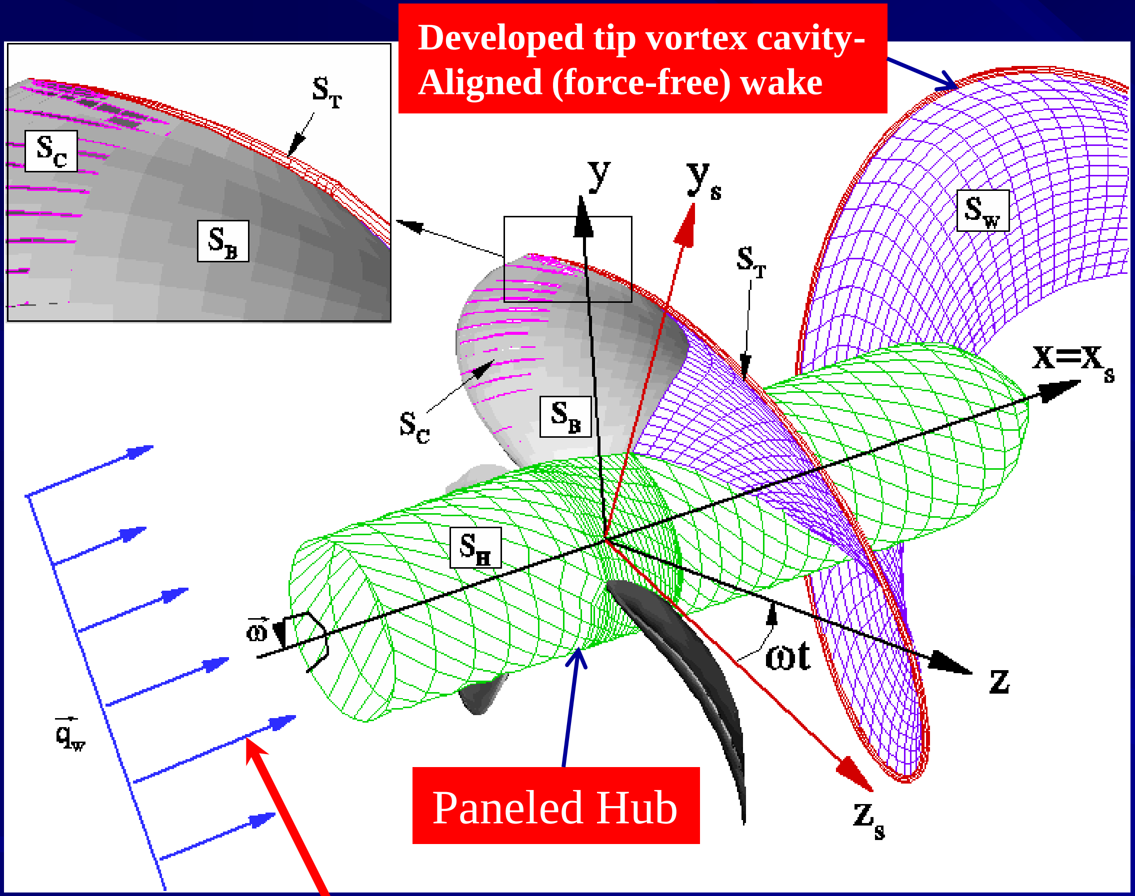

Non-axisymmetric (effective wake) inflow

- Panels are placed on **actual** blade & wake surface
- **Fully unsteady** (NOT quasi-steady)
- Solve for **unsteady** dipole strengths (**potential**) and cavity source strengths
- Determine **unsteady** pressure distributions and **sheet cavity** patterns on blade

- **PROPCAV (code name)**

What is "Effective Wake"?

- It is the local inflow to the propeller blades
- It is NOT the same as the nominal wake (inflow in the absence of the propeller), unless the inflow is uniform
- It is due to the non-linear interaction between vorticity in the inflow and that on the blade/wake
- It must be evaluated by considering the global flow (including the effect of the propeller), and must be handled by solving the Euler equations or the Navier-Stokes equations

VLM vs. BEM

The two methods VLM (MPUF-3A) and BEM (PROPCAV) produce results which are quite close to each other, especially when the following are included:

- Thickness/loading coupling (Kinnas, JSR - Journal of Ship Research - 1992)
- Leading Edge Corrections in the case of cavitating flow (Kinnas, JSR – 1991)

However, the BEM is still a more accurate method, especially at the Leading Edge and the Tip of the Blade, and thus provides a better platform for coupling the inviscid solution with an integral boundary layer solver.

Green's 3rd Identity
(using constant dipole and source distributions)

$$2\pi\phi_p(\vec{x},t) = \iint_{S_{WS}(t)\cup S_T(t)\cup S_C(t)} \left[\phi_q(\vec{x},t)\frac{\partial G(p;q)}{\partial n_q(t)} - \frac{\partial \phi_q(\vec{x},t)}{\partial n_q(t)} G(p;q)\right] dS + \iint_{S_W} \Delta\phi_w(r_q,\theta_q,t)\frac{\partial G(p;q)}{\partial n_q(t)} dS$$

- **Known on cavity**
- **Unknown on wetted blade**

- **Known on wetted surface**
- **Unknown on cavity**

Our cavity model

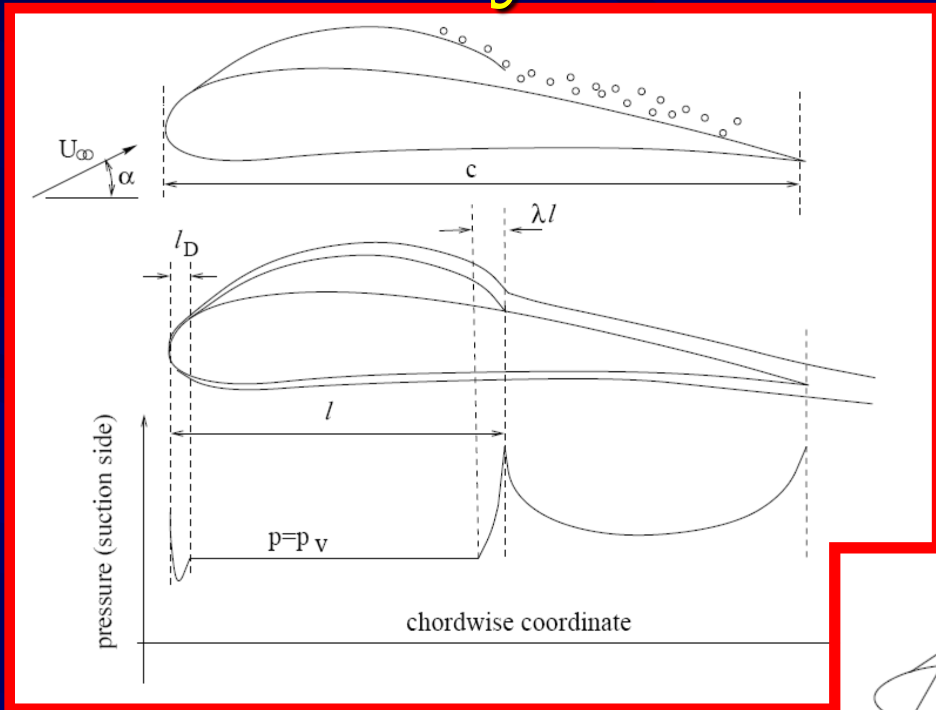

From Kinnas and Fine (Journal of Fluid Mechanics, 1993)

Other cavity models

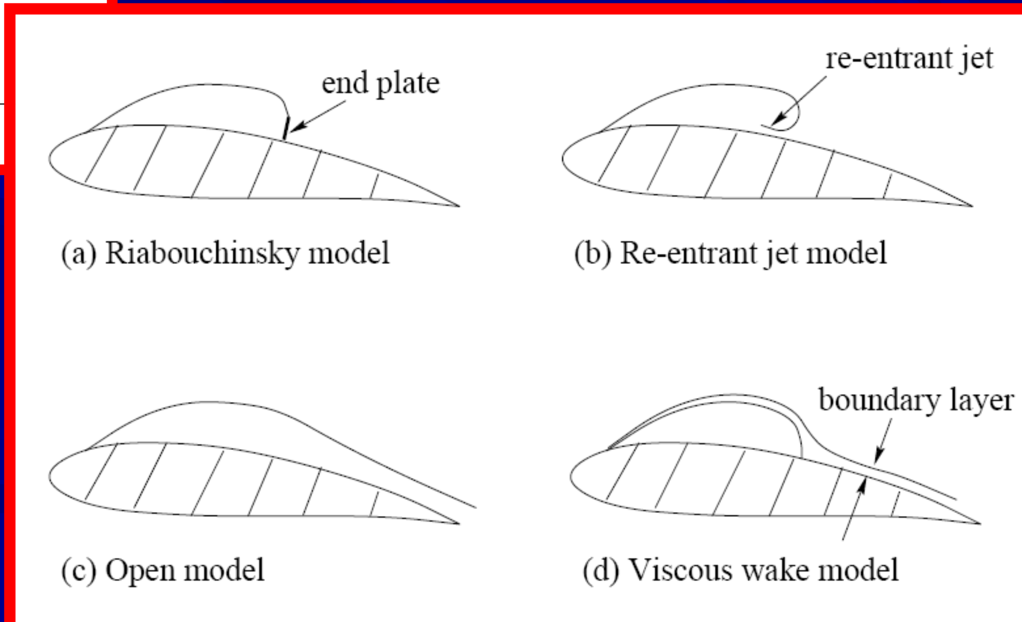

(a) Riabouchinsky model
(b) Re-entrant jet model
(c) Open model
(d) Viscous wake model

Two approaches to model sheet cavity

- **Thin cavity:** cavity panels placed **on foil** under cavity
- **Non-linear cavity:** cavity panels placed **on cavity**

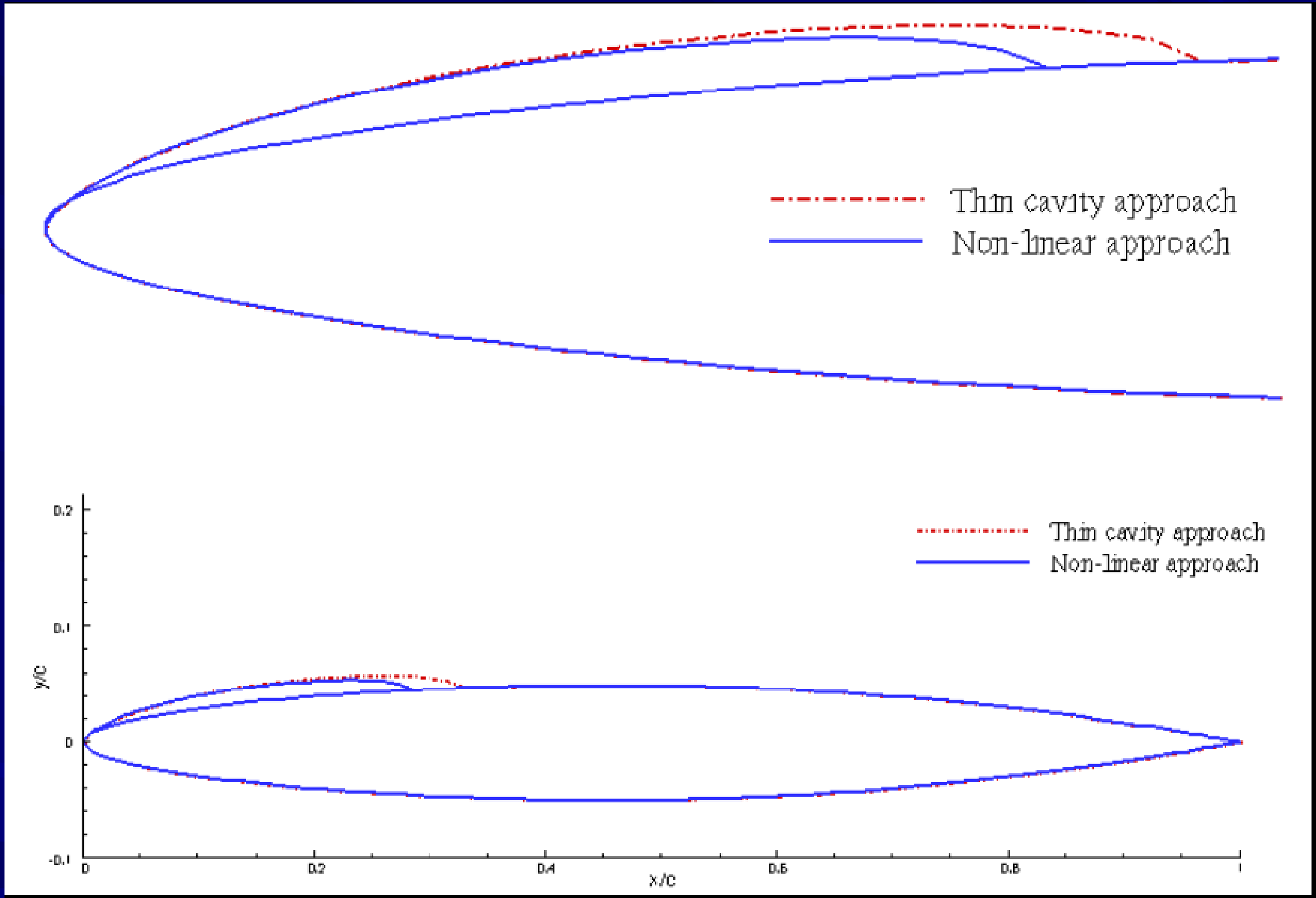

Kinnas & Fine (Journal of Fluid Mechanics, 1993)

The thin cavity approach is used in PROPCAV

How important is wake alignment?

Results from using **fully unsteady** wake alignment in PROPCAV

Blade forces for DTMB 4661 at 20º shaft inclination

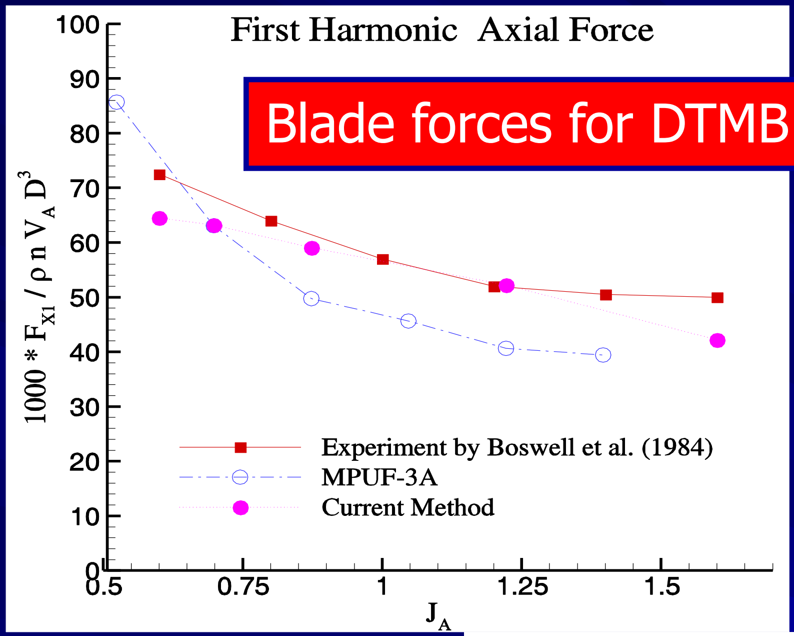

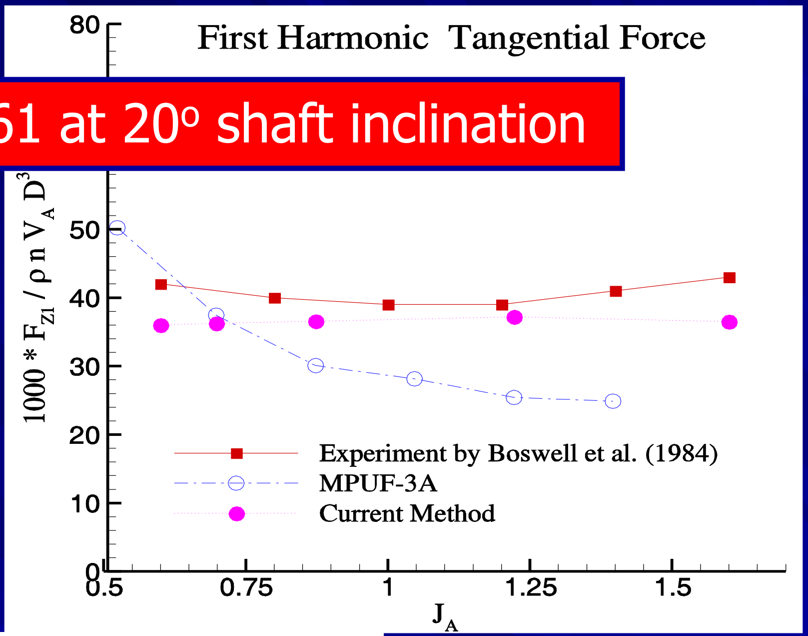

Lee H & Kinnas, S.A. JSR 2005

Shaft inclination=20 degs

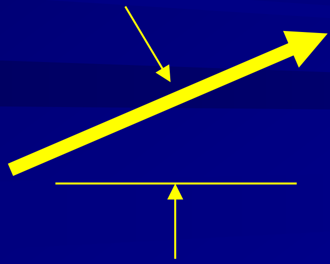

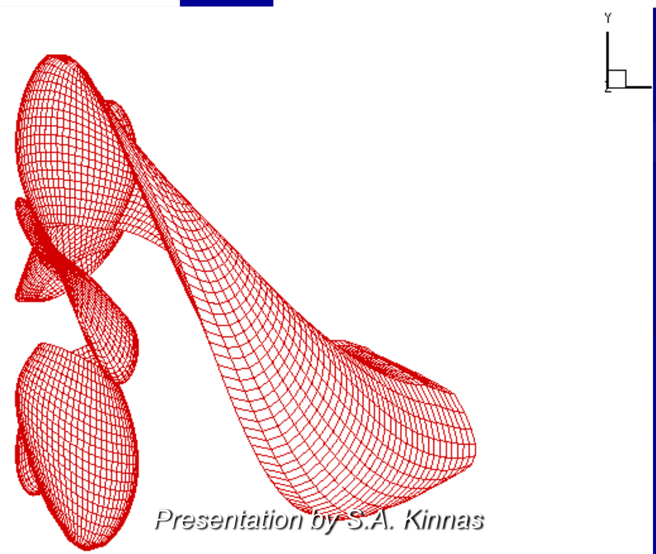

MPUF-3A uses a simplified wake alignment model which aligns (trailing) wake with the undisturbed inflow (wake)

How important are the effects of viscosity?

Included in PROPCAV via coupling with XFOIL

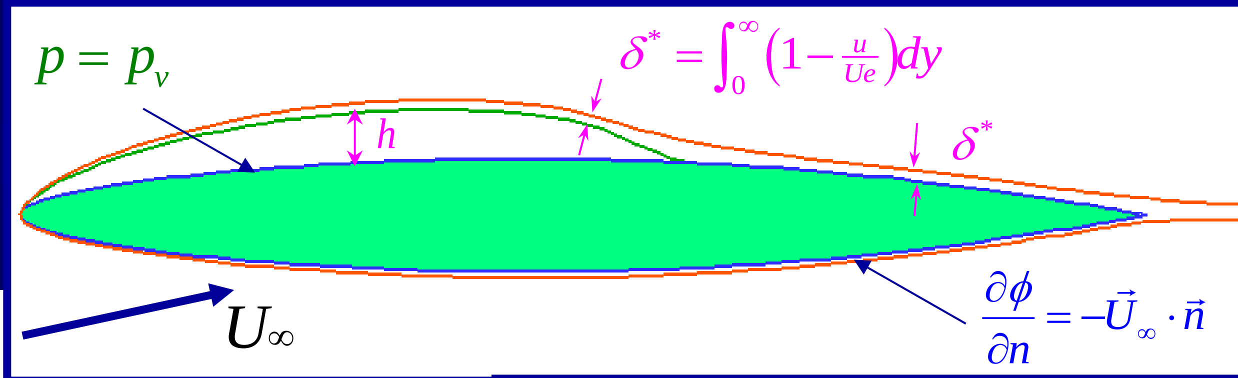

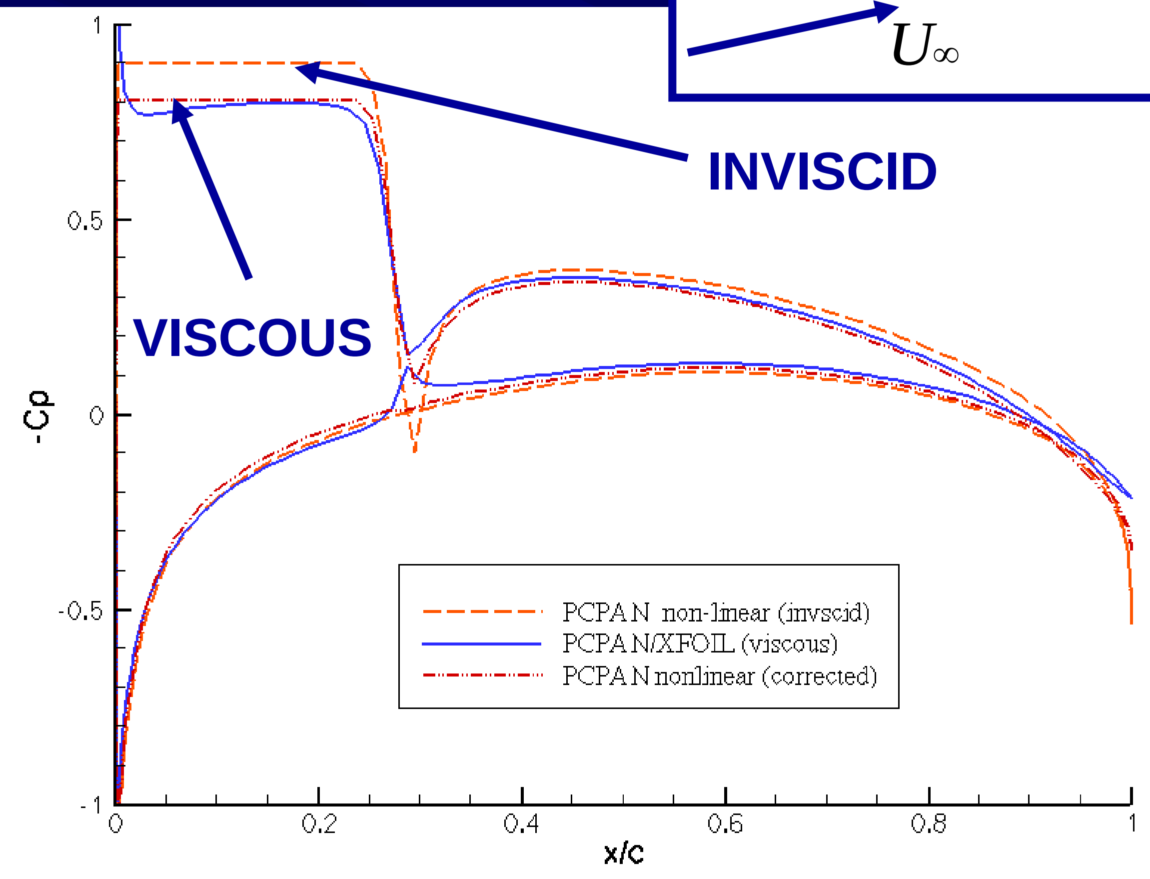

Results shown are for *fixed* cavity length

Coupling with XFOIL (a 2-D method) was applied first using 3-D inviscid pressures on each blade strip, but more recently the interaction of 3D boundary layer sources on different strips have also been included

Effect of viscosity on cavity shape for *fixed* cavitation number

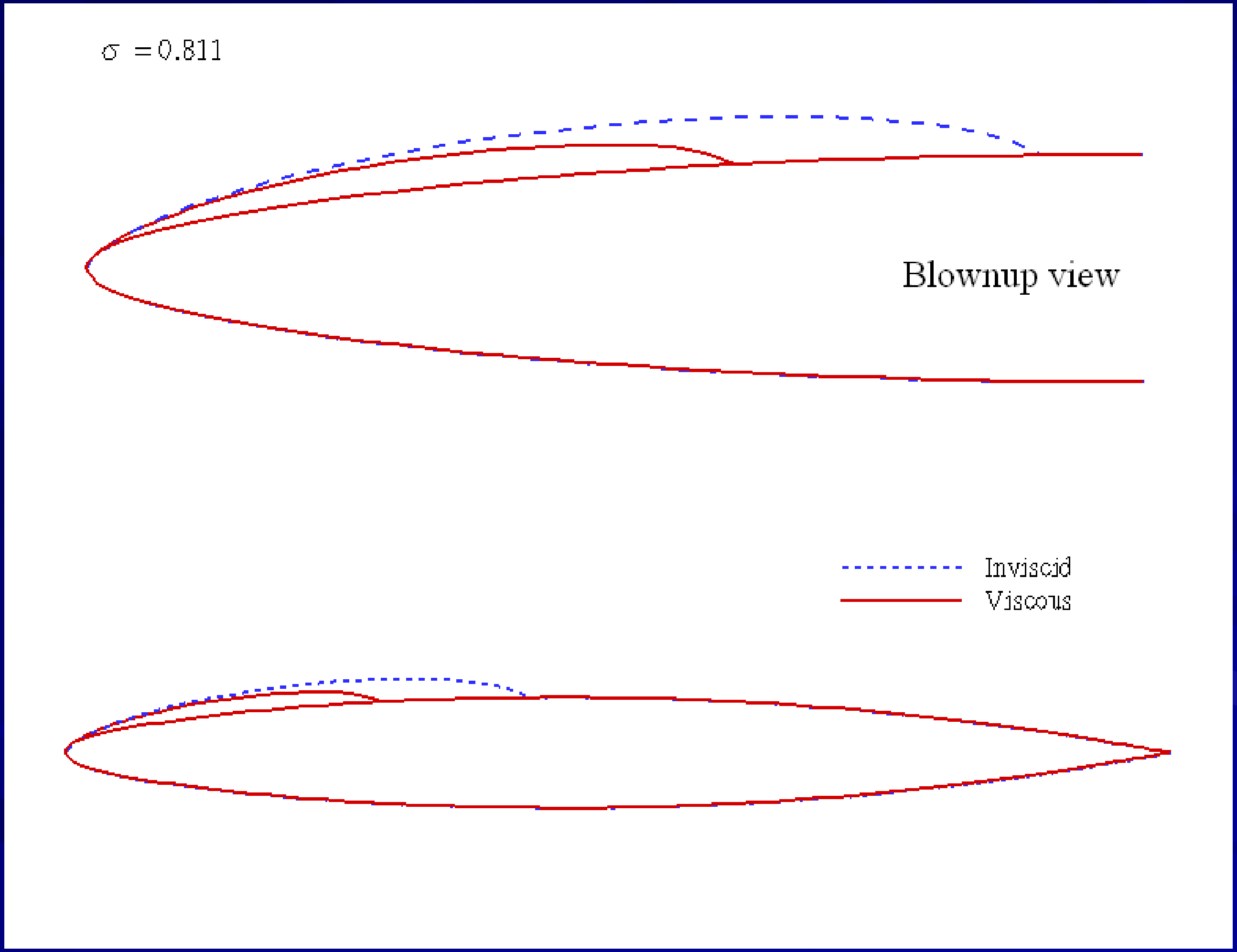

Brewer & Kinnas (Journal of Ship Research, 1997)

PROPELLER PERFORMANCE IN UNIFORM INFLOW

Propeller 4381, Js=0.5 (Design Js=0.889)

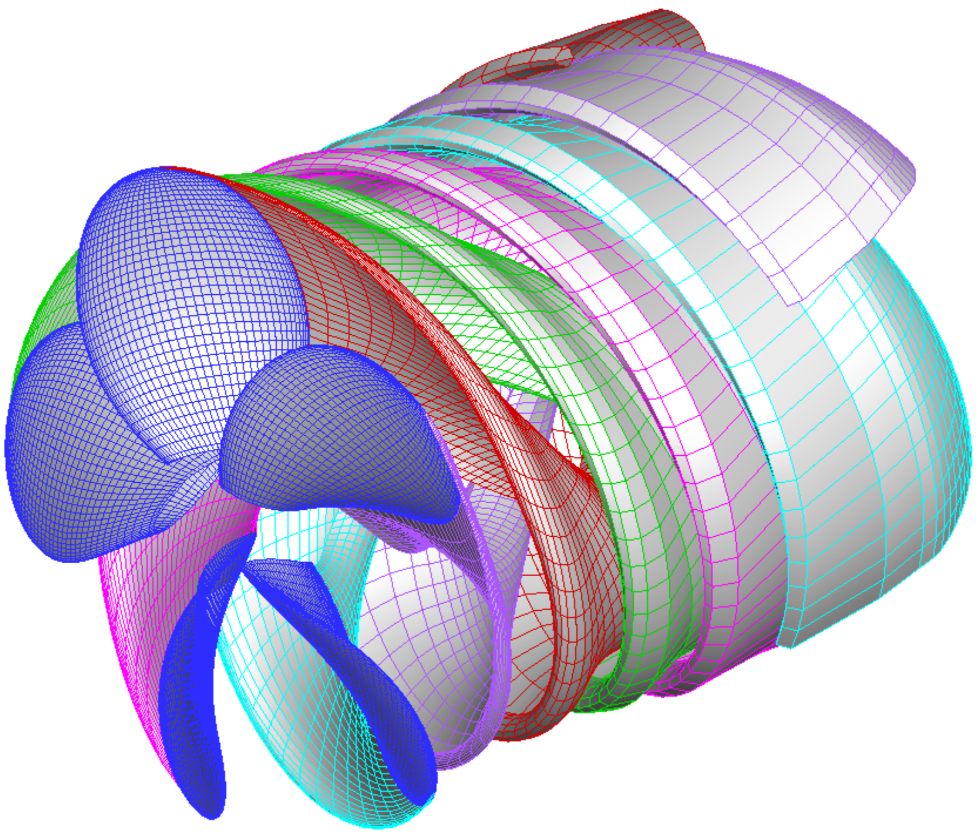

Advance Ratio Defined as: J=(Ship speed)/[(RPS)(Prop. Diameter)]

COMPARISON OF RESULTS FROM VARIOUS METHODS

- A model which can **locally correct the results from the panel method** is the goal of this study. PSF-2 Wake is a simplified/global trailing wake alignment model

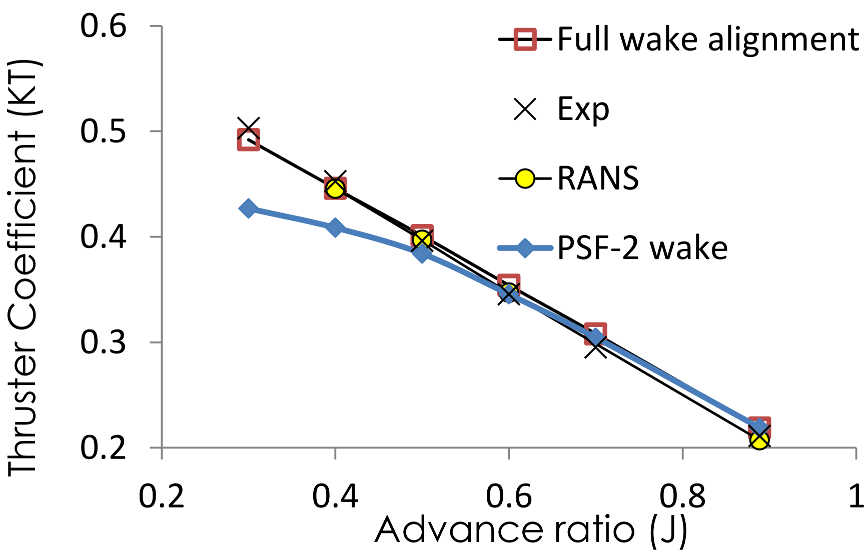

Tian and **Kinnas** (2012) , *A Wake Model for the Prediction of Propeller Performance at Low Advance Ratios.* International Journal of Rotating Machinery

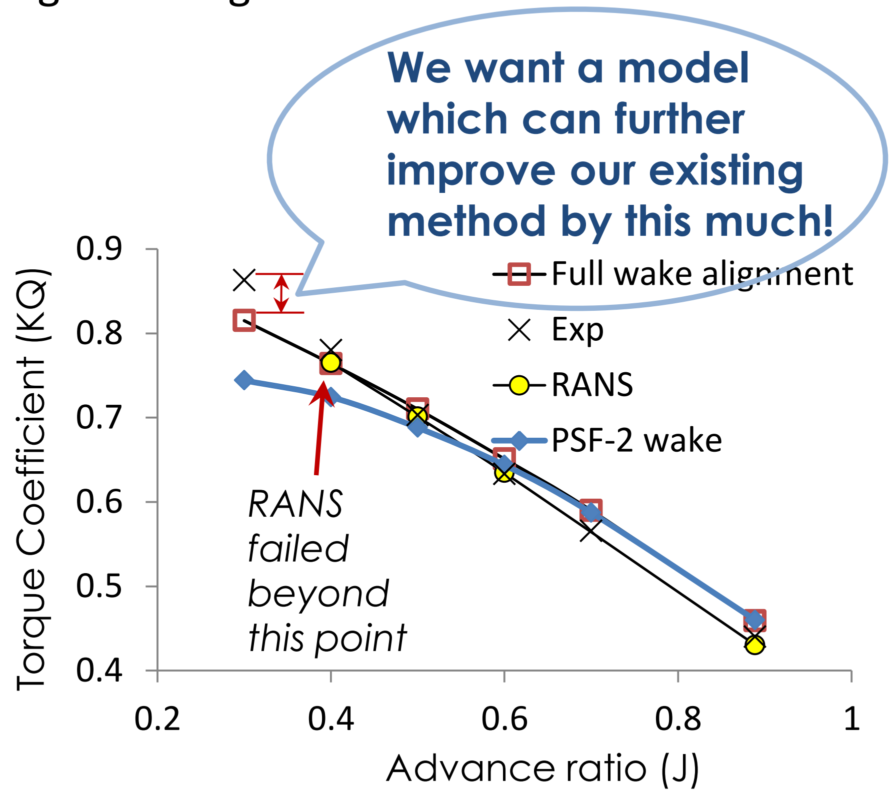

Panel method : 5 mins on a Laptop

RANS: 8 hrs on 24 CPUs.

Q: How to interact with solid boundaries (ships' hull, hub, duct, pod, water-jet casing) or other blade rows (in the case of contra-rotating propellers, stator/rotor pair, of twin podded props)?

(Our) A: Still model the blades using MPUF-3A or PROPCAV. The effect of the "other bodies" or "other blades" is then handled via a generalization of the concept of "effective wake"="total flow" – "flow induced by blade itself". The total flow is determined via an Euler or RANS solver in which the blade is represented with a distribution of body forces (="sources" in the momentum equations). An iterative process is then formulated.

Improved Effective Wake Calculation

(coupling MPUF-3A via PF2NS with Fluent)

Kinnas et al (ISOPE'12, SMP'13), Tian et al (JSR 2014), Tian & Kinnas, (Journal of OMAE 2015)

PFS2NS:code for coupling between Potential Flow and Navier-Stokes solvers

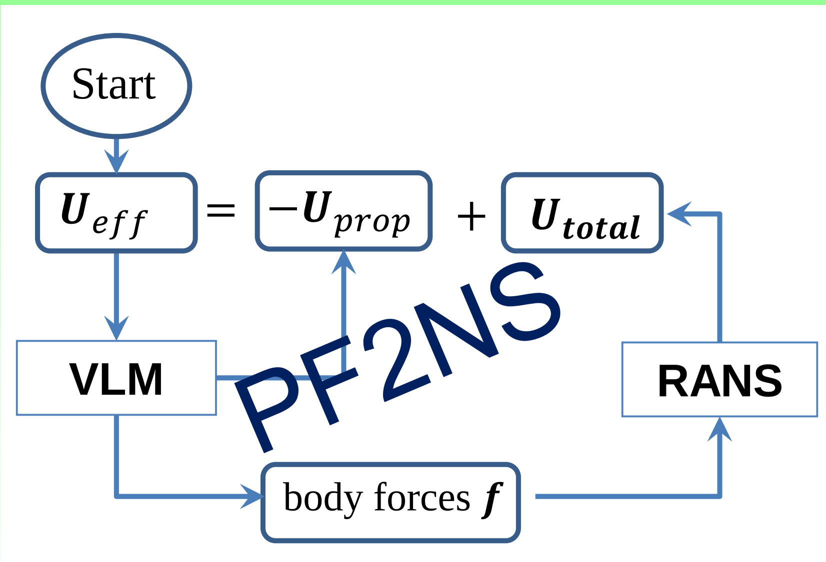

CIS: Conservative Interpolation Scheme

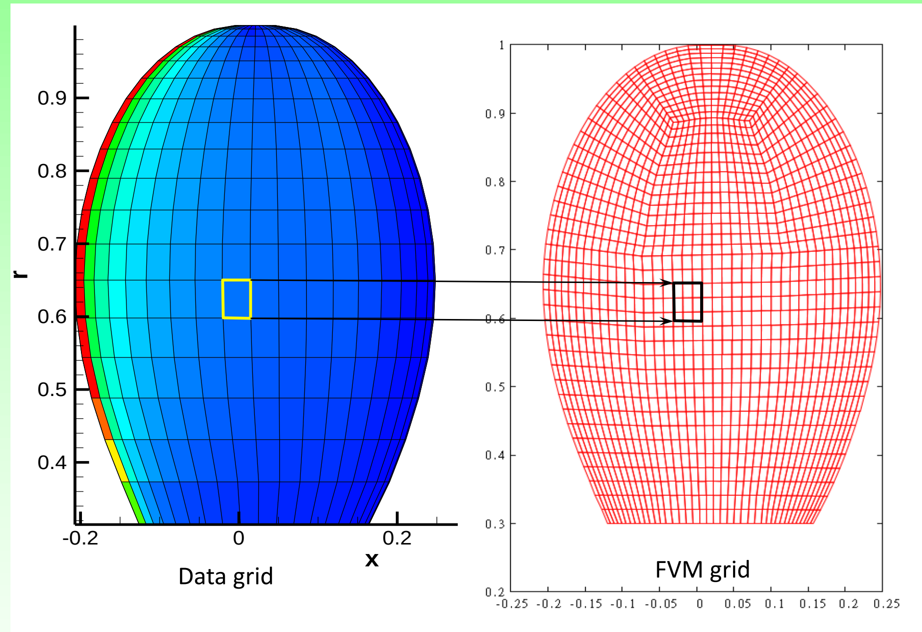

Grid in MPUF-3A   Grid in RANS

VLM: MPUF-3A

RANS: Fluent, OpenFOAM, NS-3D

Duct with blunt T.E.

Streamlines for J_S=0.7

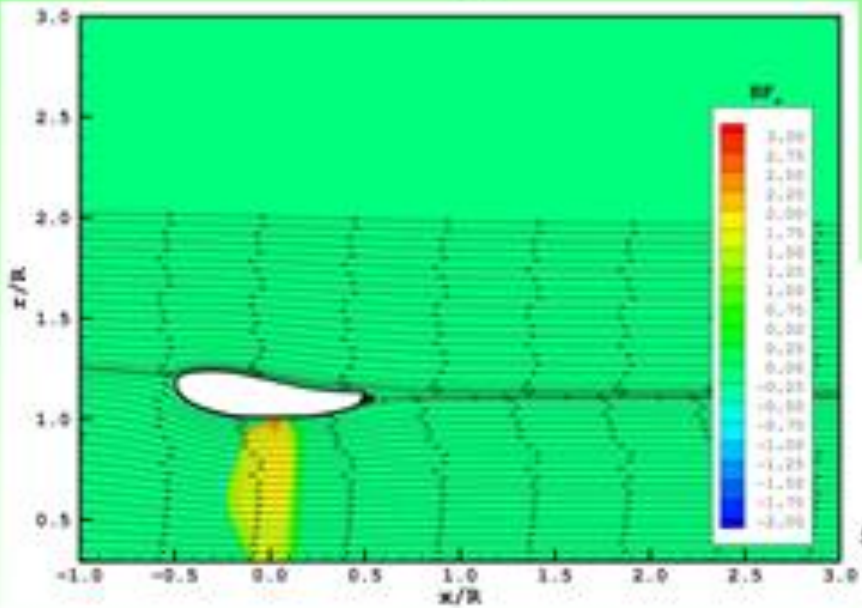

Streamlines for J_S=0.2

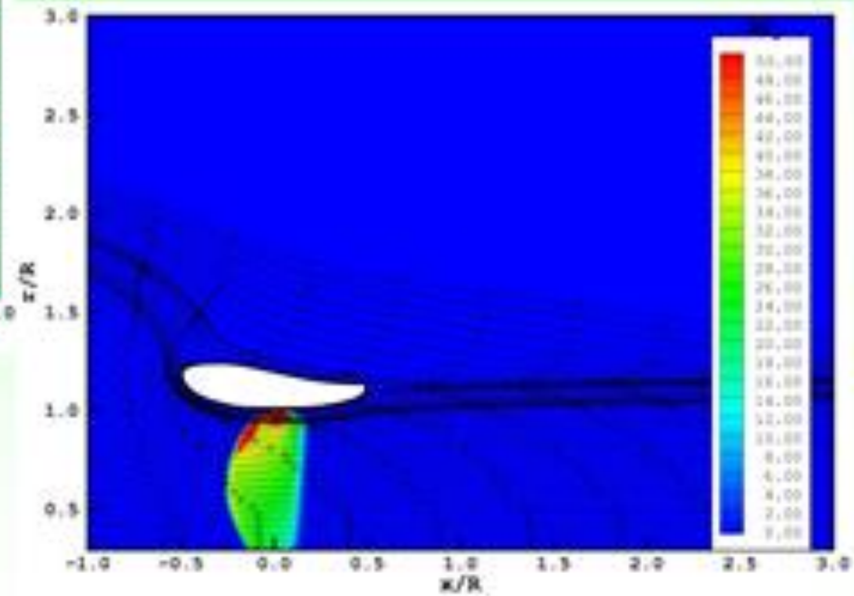

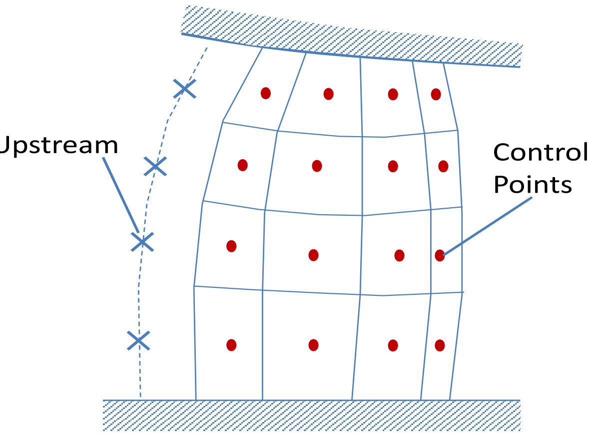

Prediction of Performance

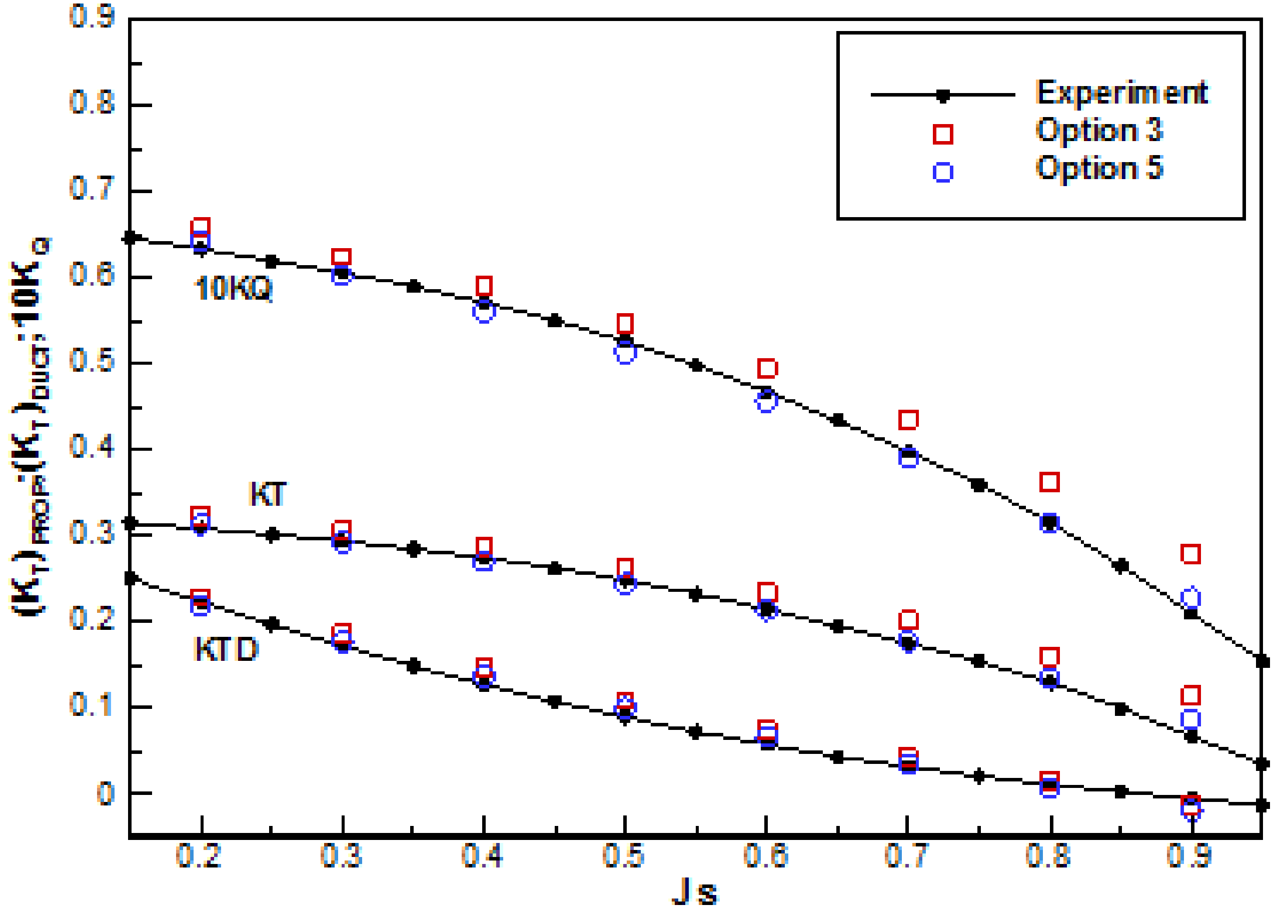

- Option 3: effective wake evaluated upstream of blade
- Option 5: effective wake evaluated at control points
- From Tian et al (JSR 2014)

CORRELATION OF MPUF-3A/FLUENT WITH STAR-CCM+ AND FLUENT

- MPUF-3A/FLUENT method is applied to the case of Dyne ducted propeller, the design advance ratio of which is around 0.40.
- Fully 3-D viscous simulation are conducted in both *Star-CCM+* and Fluent for correlations.

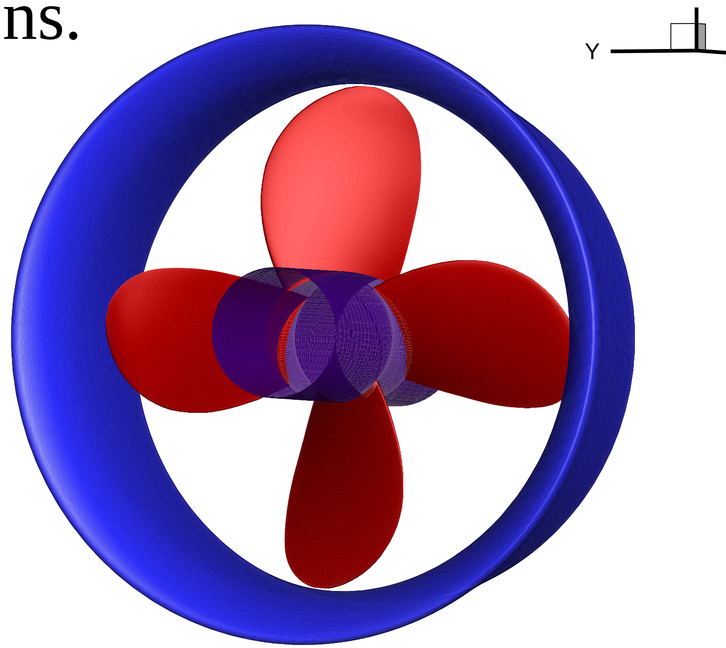

Mesh conditions in fully 3-D viscous simulation

- Polyhedral cells and hexahedral cells are respectively utilized in the rotating region and static region.
- Periodic interfaces are applied, making only a quarter of the whole domain necessary for the simulation.

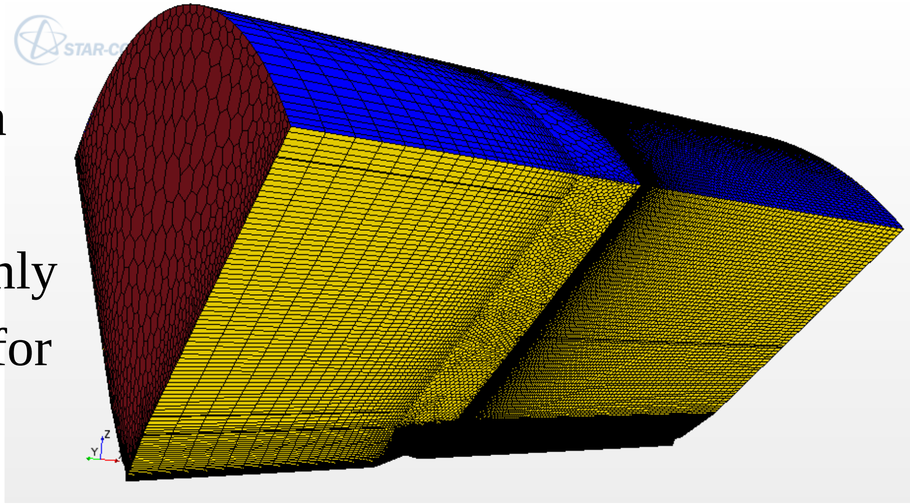

mesh of periodic domain

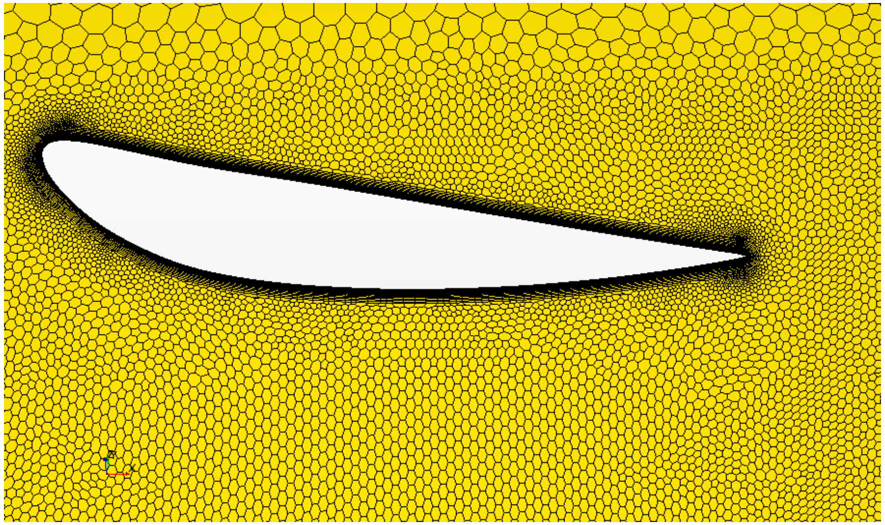

mesh around duct

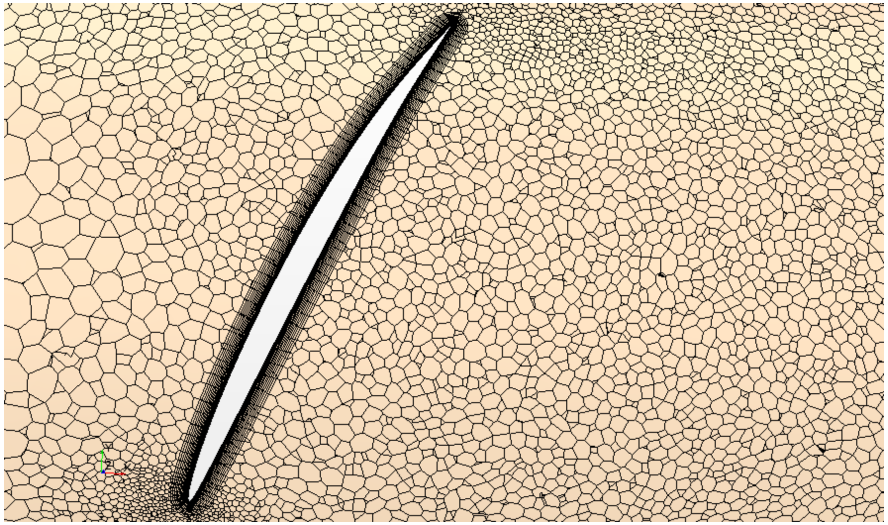

mesh around blade station r/R=0.60

Results-Ducted Propeller with Sharp Trailing Edge Duct

The force predicted by the present hybrid method agree very well with that from the full-blown RANS simulations and also with experiment.

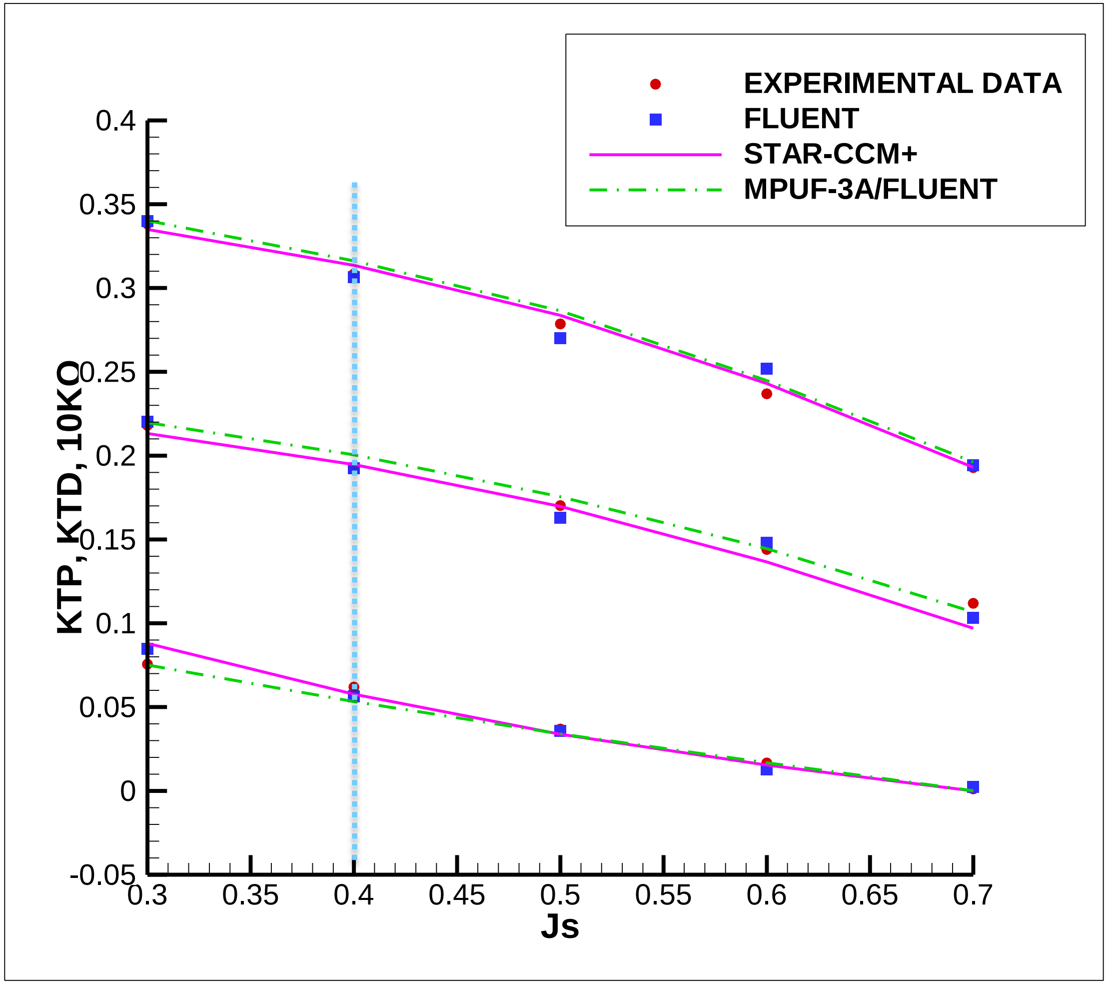

Results-Ducted Propeller with Sharp Trailing Edge Duct

- Correlation of the pressure distribution on the blade and duct are made hereafter. For each loading condition, two different blade stations, 0.65 (mid-station of the blade), 0.80 (near the tip) are selected for comparison.
- The pressure distribution on the duct must be circumferentially averaged before correlation.

Results-Ducted Propeller with Sharp Trailing Edge Duct

J=0.30 High loading

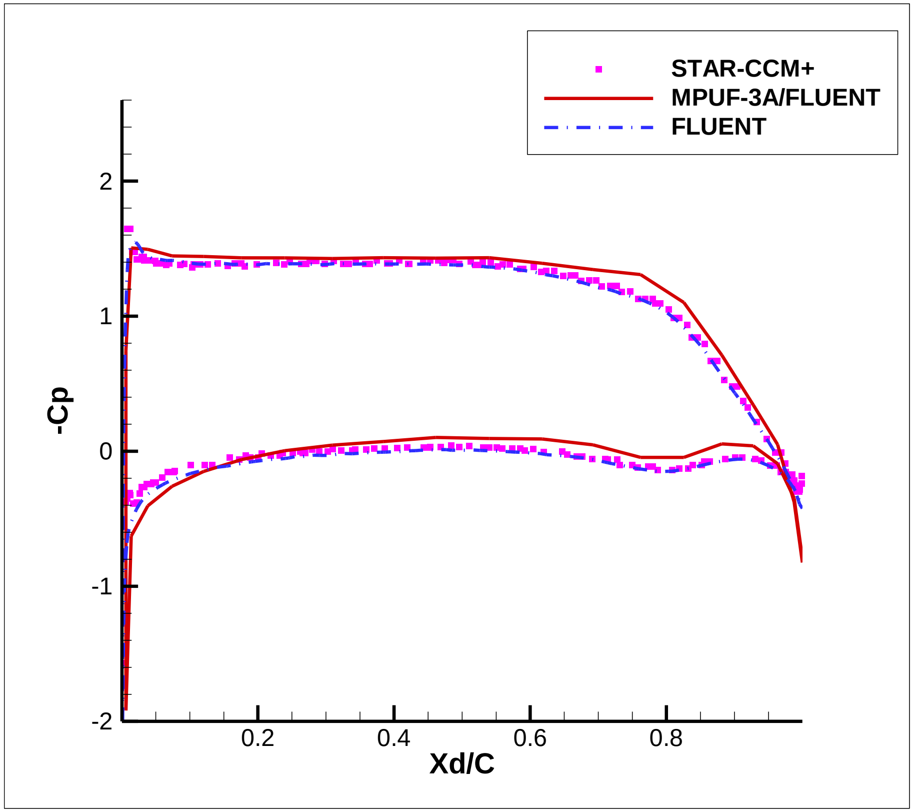

blade station r/R=0.65

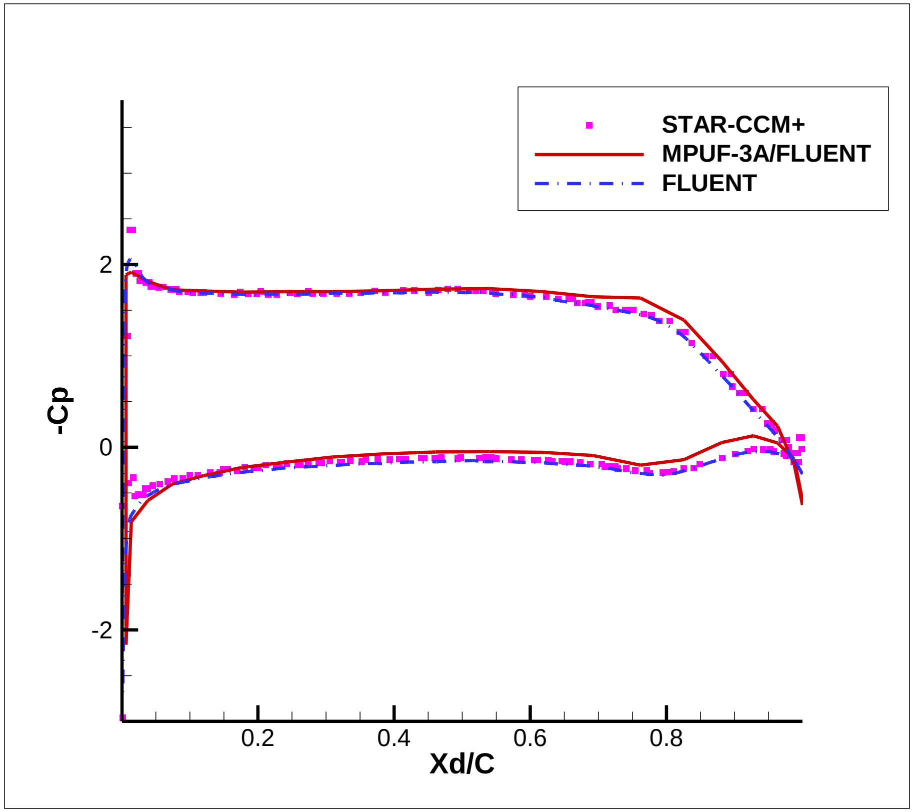

blade station r/R=0.80

Results-Ducted Propeller with Sharp Trailing Edge Duct

***J*=0.30** High loading

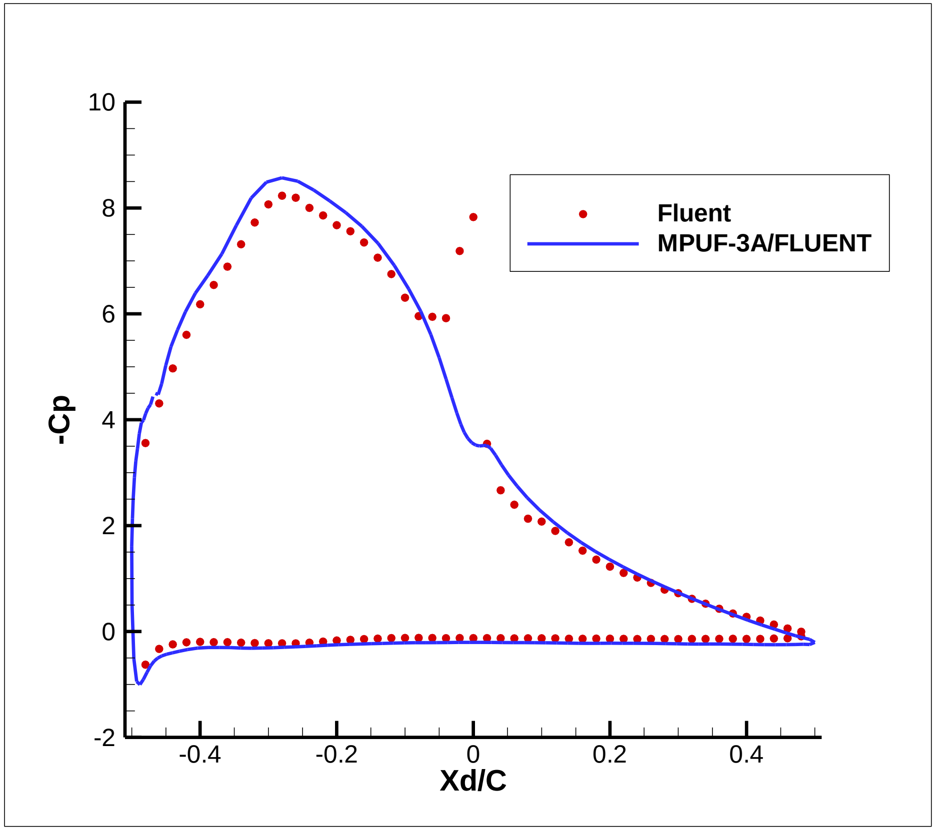

Circumferentially averaged pressure on duct

Results-Ducted Propeller with Sharp Trailing Edge Duct

***J*=0.40** design loading

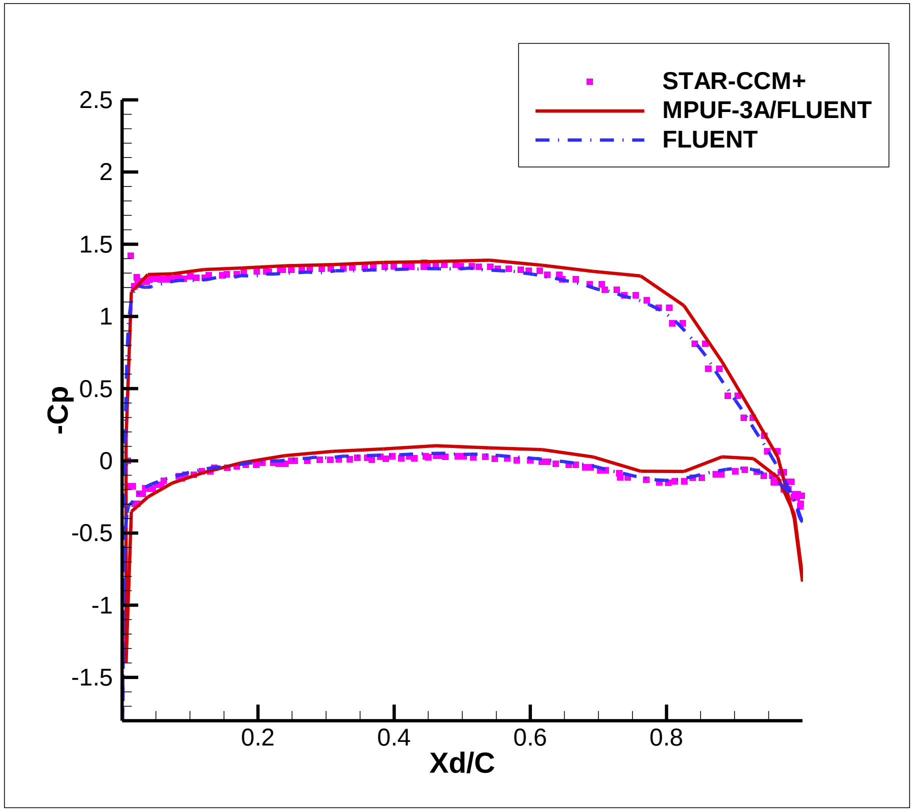

blade station r/R=0.65

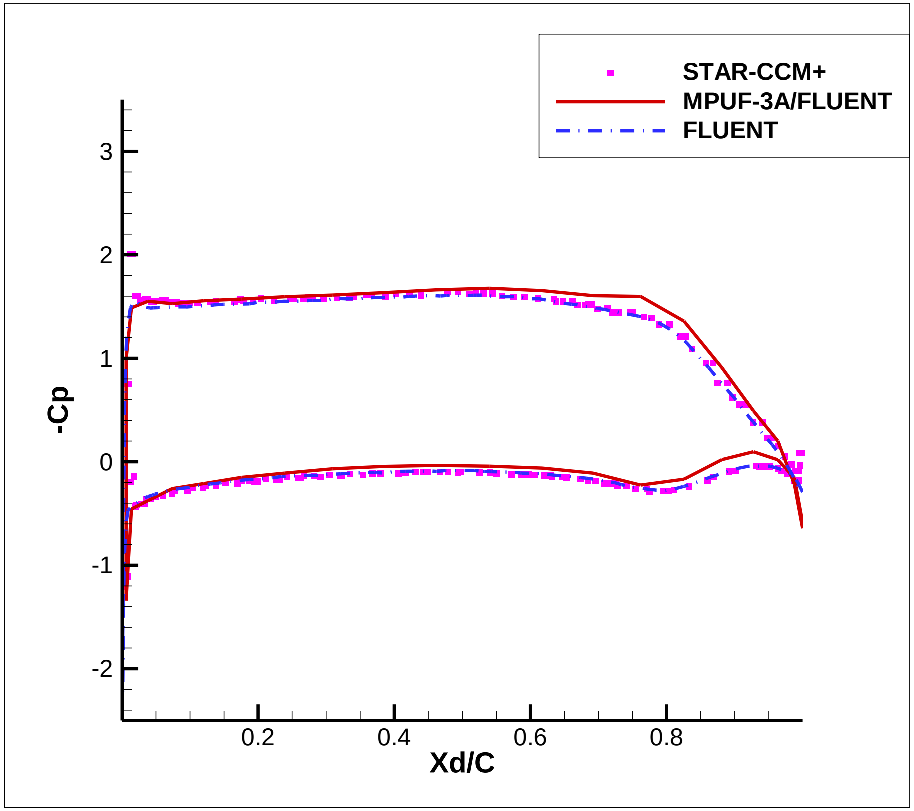

blade station r/R=0.80

Results-Ducted Propeller with Sharp Trailing Edge Duct

***J*=0.40** design loading

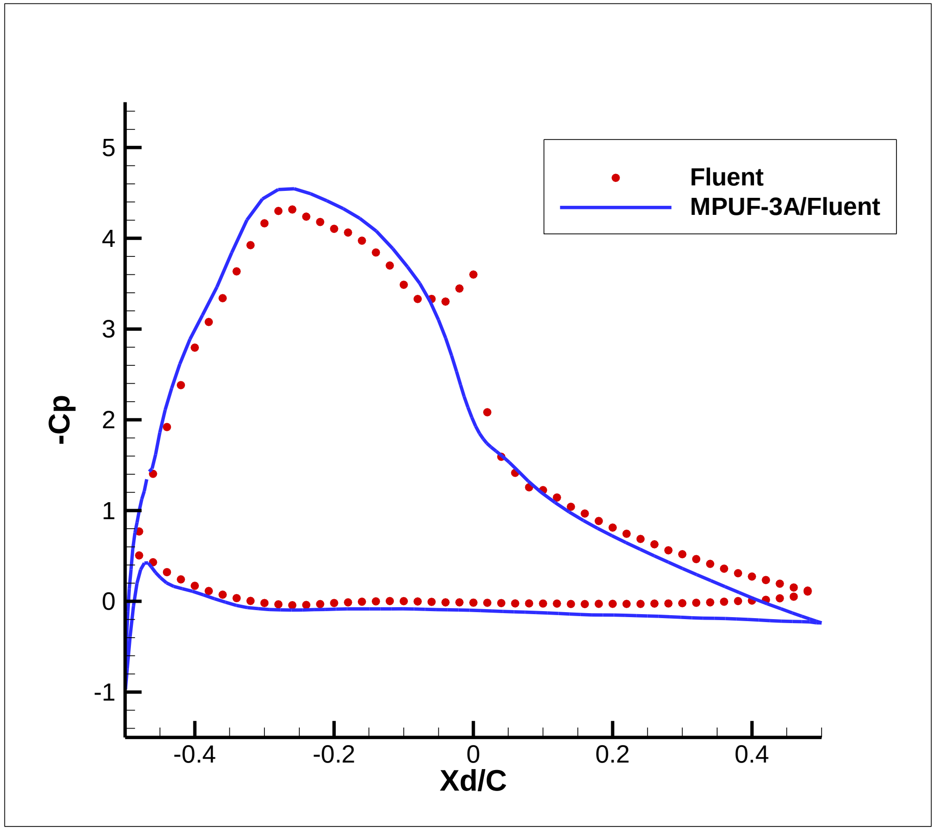

Circumferentially averaged pressure on duct

Results-Ducted Propeller with Sharp Trailing Edge Duct

Comparison of Efficiency

Method	***Star-CCM+***	***ANSYS Fluent***	**MPUF-3A /Fluent**
Cell No.	3.2 million	6.9 million	25,550
Reynolds No.	1.0e+6	1.0e+6	1.0e+6
Turbulence Model	*k-ε*	*k-ε*	*k-ε*
Total running time	Over 30 hours (32 CPUs)	Over 30 hours (32 CPUs)	30 minutes (8 CPUs)

Extension if the case of internal Water-jet flows

Background

- Axial flow water-jets are propulsors promising to provide a balance between the robustness and performance particularly suited to high-speed marine vessels.
- Inducers are widely used in rocket engine turbo pumps to prevent cavitation in the pump main stages therefore permitting higher turbo pump operating speeds and reduced pump inlet pressure.

Motivation

- Complex geometry configurations and inevitable cavitation due to local pressure depression make simulation and analysis of flow inside water-jet or inducer pump considerably challenging.

Objectives

- To predict hydrodynamic performance and thrust/torque breakdown due to super cavitation inside a water-jet pump.
- To predict hydrodynamic performance of the generic inducer and the inducer given by the industry.

Methodology (Inviscid Water-jet/Inducer Model)

- **Panel Method (details in Sun, PhD/OEG'08, Sun & Kinnas, SNAME Trans. '08, Chang, PhD/OEG'12, Chang & Kinnas, SNH/ONR 2012)**
  - Assuming the fluid inside a water-jet is irrotational, incompressible and inviscid. (potential flow theory applied)
  - The total inflow relative to the propeller:
    $$\vec{V}_{in}(x,y,z,t)=\vec{U}_w(x,r,\theta-\omega t)+\vec{\omega}\times\vec{x}$$
    $\vec{U}_w$ is the effective inflow in the ship fixed coordinate system.
    $\vec{\omega}$ is a constant angular velocity vector.
  - The total velocity in the rotating coordinate system:
    $$\vec{q}_t(x,y,z,t)=\vec{V}_{in}(x,y,z,t)+\nabla\phi(x,y,z,t)$$
  - The perturbation potential satisfies the Laplace's equation in the fluid domain.
    $$\nabla^2\phi(x,y,z,t)=0$$

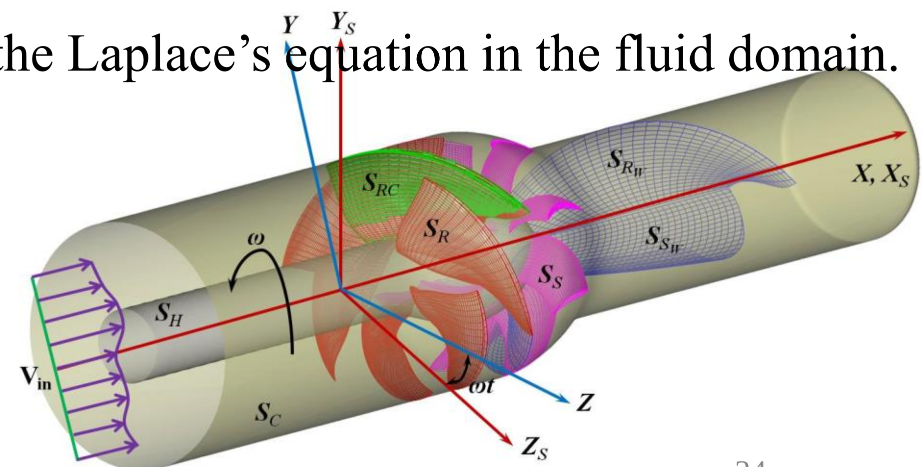

Methodology (Inviscid Water-jet/Inducer Model)

Panel Method

- Applying Green's third identity with respect to the perturbation potential ϕ at any time, the Governing Equation is: (for both rotor and stator)

$$2\pi\phi_P(t) = \int_{S_R+S_{RC}} \left[\phi_q(t)\frac{\partial G(p;q)}{\partial n_q} - G(p;q)\frac{\partial \phi(t)}{\partial n_q} \right] ds + \int_{S_{R_W}} \Delta\phi_{R_W}(t)\frac{\partial G(p;q)}{\partial n_q} ds$$

$$+ \int_{S_S+S_{SC}} \left[\phi_q(t)\frac{\partial G(p;q)}{\partial n_q} - G(p;q)\frac{\partial \phi(t)}{\partial n_q} \right] ds + \int_{S_{S_W}} \Delta\phi_{S_W}(t)\frac{\partial G(p;q)}{\partial n_q} ds$$

$$+ \int_{S_{HC}} \left[\phi_q(t)\frac{\partial G(p;q)}{\partial n_q} - G(p;q)\frac{\partial \phi(t)}{\partial n_q} \right] ds$$

Interaction between rotor and stator is time-averaged

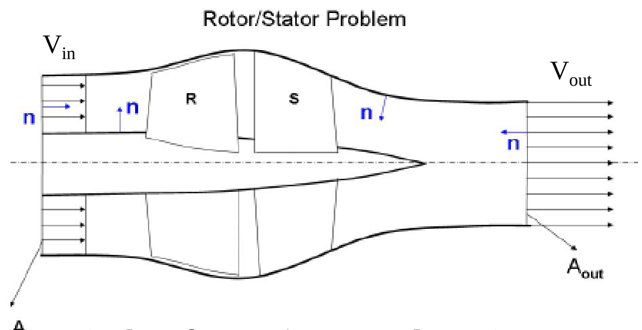

(Taken from Kinnas et al.2007)

Methodology (Inviscid Water-jet/Inducer Model)

Boundary Conditions

- The flow is tangent to the wetted rotor blades, hub and casing surfaces.

$$\frac{\partial\phi}{\partial n} = -\vec{V}_{in}(x,y,z)\cdot\vec{n}$$

- The Morino's [Morino and Kuo, 1974] steady Kutta condition is applied to ensure the fluid velocities are finite at the trailing edge of the blade. An iterative pressure Kutta (IPK) condition [Kinnas and Hsin, 1992] is required to force a zero pressure jump between the pressure and suction sides at the blade trailing edge.

- The dynamic boundary condition on the blade cavity:

$$|q_t|^2 = n^2D^2\sigma_n + |\mathbf{V}_{in}|^2 + \omega^2r^2 - 2gy_s - 2\frac{\partial\phi}{\partial t} \qquad \textit{cavity number } \sigma_n = \frac{P_o - P_v}{0.5\rho n^2 D^2}$$

r: distance from the axis of the rotation; g: gravitation constant; y_s: vertical distance from the horizontal plane through the axis; n: rotating frequency; D: propeller diameter.

- The kinematic boundary condition on cavity:

$$(\frac{\partial}{\partial t} + q_t\cdot\nabla)[n - h(s,v,t)] = 0 \quad h = \textit{cavity} \text{ height}$$

- The cavity detachment location is determined iteratively to satisfy the *smooth detachment conditions* (Young & Kinnas[JFE, 2001] and Young [2002]).

- The cavity closure condition implies that the cavity needs to be closed at the end of the cavity.

Methodology (Inviscid Water-jet/Inducer Model)

Boundary Conditions (Inlet and Outlet Boundaries)

- The flow at the inlet should be equal to the inflow, thus:

$$\left.\frac{\partial \phi}{\partial n}\right|_{in} = \nabla \phi \cdot \vec{n} = 0$$

- The flow at the outlet of the casing has to satisfy the continuity equation, thus:

$$\left.\frac{\partial \phi}{\partial n}\right|_{out} = V_{in} - V_{out}$$

$$where \quad V_{in} \cdot A_{in} = V_{out} \cdot A_{out} \Rightarrow V_{out} = V_{in} \frac{A_{in}}{A_{out}}$$

- When solving the BVP of the internal flow, the perturbation potentials at the inlet are set to **zero** to make the solution unique.

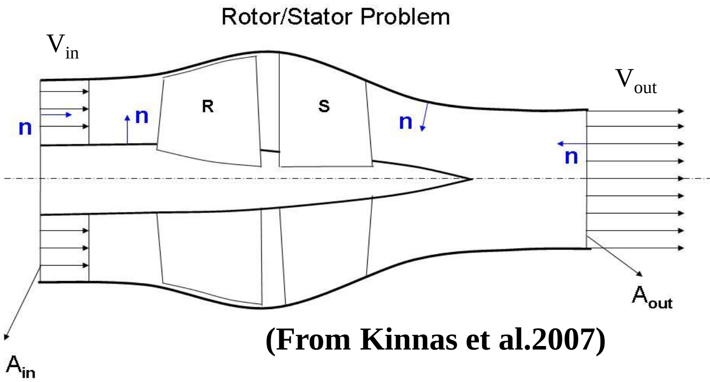

(From Kinnas et al.2007)

Main characteristics of the present method

- **Inviscid –Fully Unsteady-Cavitating– Based on low-order perturbation potential method**

- **Cavity model searches for face and back cavities of the corresponding detachment locations**

- **Effects of viscosity on the blades are evaluated:**
  (a) via friction coefficient C_f [f(Re)] and empirical viscous pitch correction, or
  (b) via coupling with a boundary layer solver (XFOIL)

Previous Research

Tip Gap Model

- Orifice flow theory: Kerwin et al. (1987) and applied in panel methods by Hughes (1993; 1997), Moon et al. (2002), and Gaggero et al. (2009).
- Tip leakage model: Gu (PhD/OEG 2006), using vortex lattice method coupling with a Euler solver to predict the influence of the viscous gap region on the overall performance of ducted propellers, and the discharge coefficient is based on the calculation of a RANS solver.

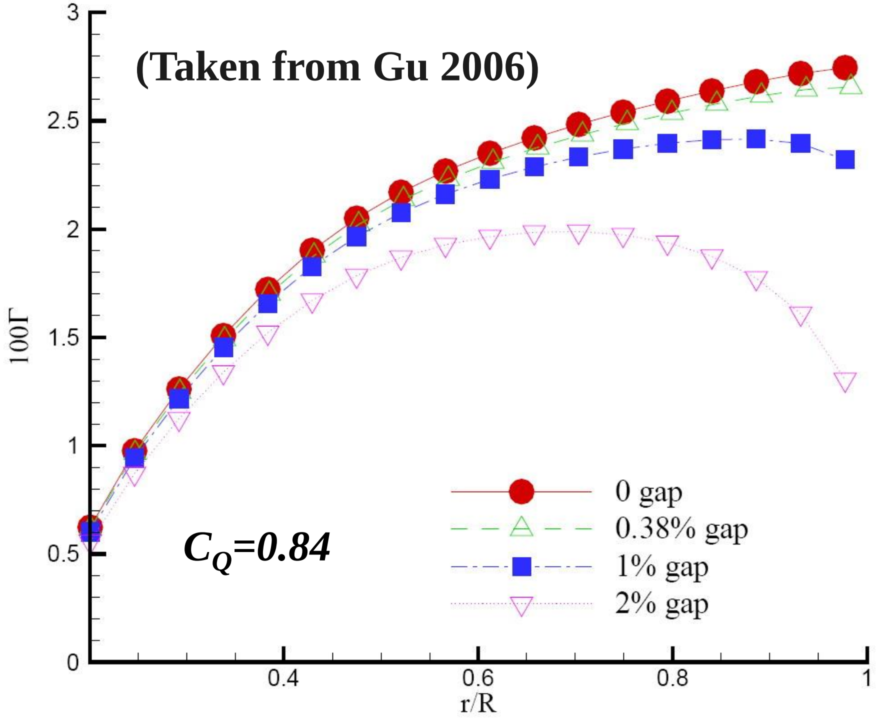

Methodology (Tip Gap Model)

Bernoulli's obstruction theory

- The flow rate, Q, through the shown orifice (gap), including the effects of viscosity, can be defined in terms of an empirically determined discharge coefficient (C_Q) :

$$C_Q = \frac{Q}{h}\sqrt{\frac{\rho}{2\Delta p}}$$

$\Delta p = p_1 - p_2$ is the difference in pressure across the gap, h is the gap height and ρ is the fluid density.

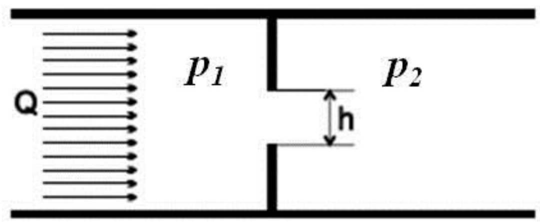

- The mean velocity V_{gap} through the gap at a given chordwise location can be expressed as:

$$V_{gap} = C_Q\sqrt{\frac{2\Delta p}{\rho}} = C_Q\left|\vec{V}_{in}\right|\sqrt{\Delta C_P}$$

and ΔC_P is the pressure coefficient on the blade tip, defined as: $\Delta C_P = \dfrac{p_1 - p_2}{\frac{1}{2}\rho\left|\vec{V}_{in}\right|^2}$

Methodology (Tip Gap Model)

Bernoulli's obstruction theory

- To incorporate the gap model into the panel method scheme, an additional row of panels will be needed to close the gap. In the kinematic boundary condition, the sources strength in the gap zone can be written as:

$$\frac{\partial \phi_q}{\partial n_q} = -\vec{V}_{in} \cdot \vec{n}_q + C_Q \left|\vec{V}_{in}\right| \sqrt{\Delta C_P} (\vec{n}_q \cdot \vec{n}_{camber})$$

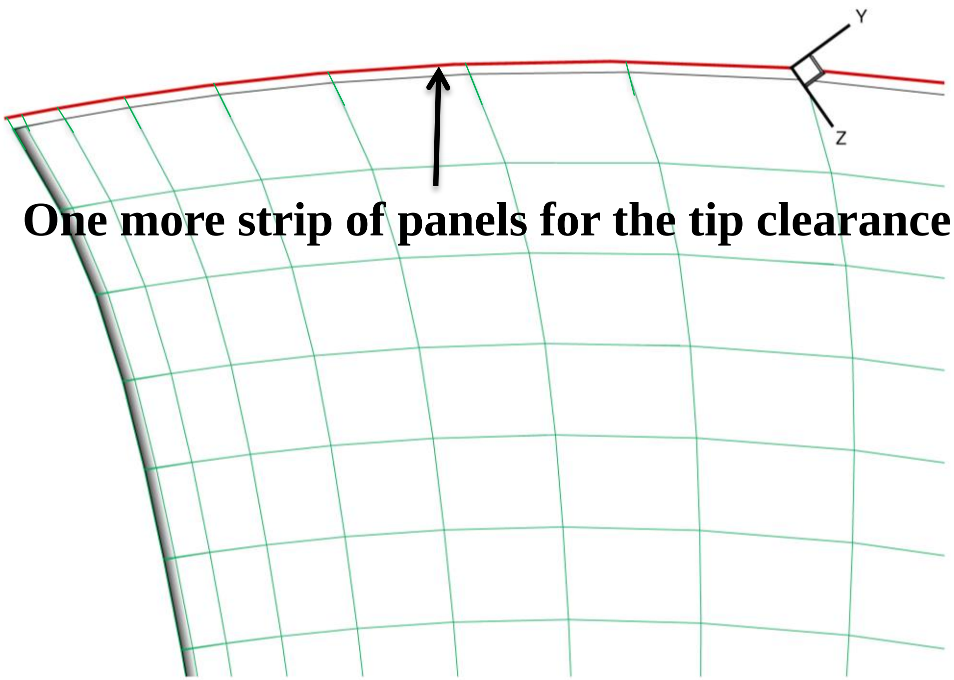

One more strip of panels for the tip clearance zone

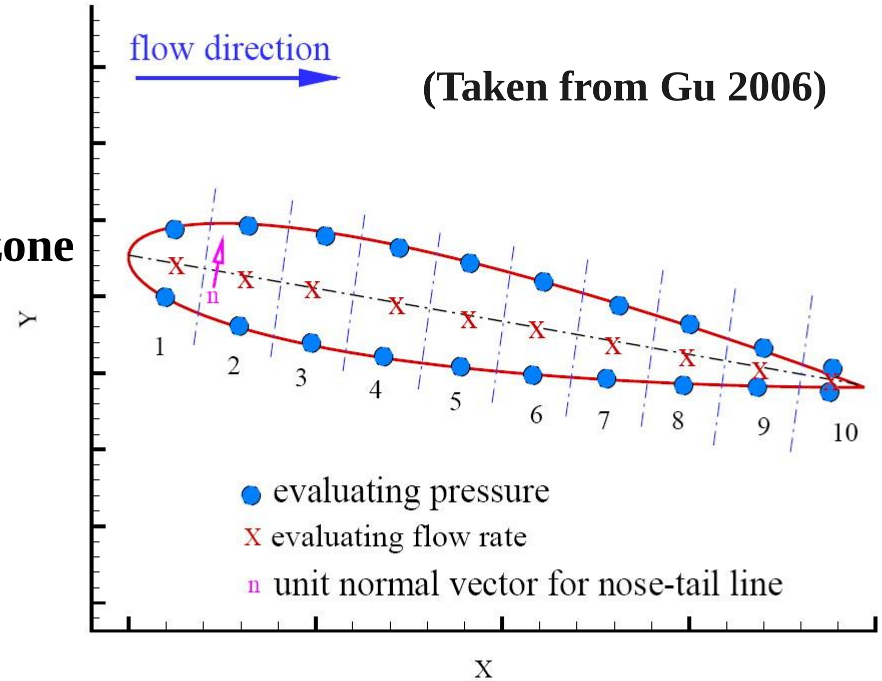

(Taken from Gu 2006)

In Hughes and Gu's theses, C_Q=0.84 is used. However, we now can determine C_Q from experimental measurement at JHU or from RANS.

Numerical Results (ONR AxWJ-2 Water-jet Pump)

Experimental (at Johns Hopkins) and Numerical Set-ups:

- The geometry of the pump and the experimental data are obtained from NSWCCD (Dec., 2009).
- The design advance ratio J_S is **1.192** and the rotational frequency is **1400** *rpm* for fully-wetted operation and **2000** *rpm* for cavitating operation at flow coefficient Q^*= **0.85**.
- Panel method: Rotor (60x20), no. of circumferential elements: 20; shroud: (-3.0, 6.03); hub (-3.0, 2.1); wake length: 4.5 R_{prop}.

Rotor **Stator**

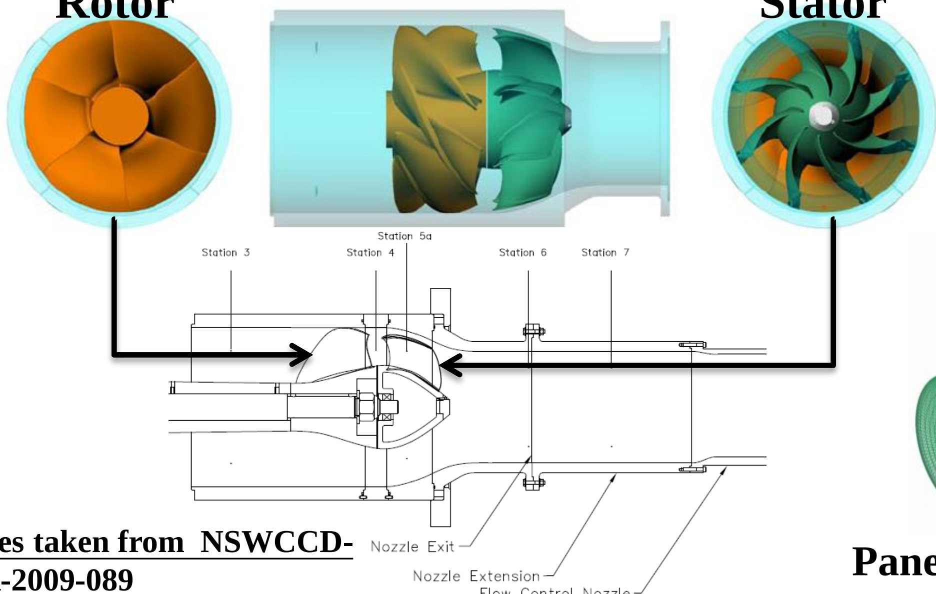

Pictures taken from NSWCCD-50-TR-2009-089 page 2 (upper) and 3 (lower)

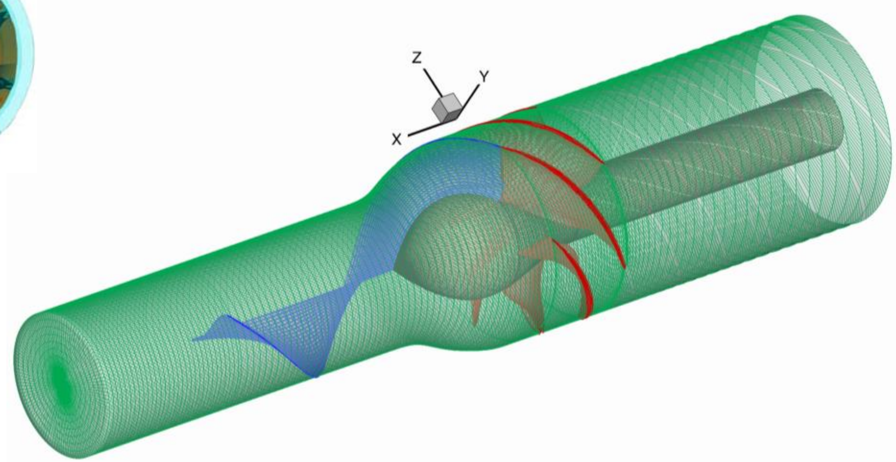

Paneled geometry for the rotor problem; the stator effect is not included in this research

Numerical Results (Rotor Only)

Numerical settings in RANS:

- 3D **Periodic** version (Rotor only): **3.07 million** cells.
- Turbulence model:
  - **k-ω SST**.
  - y^+: 40~180 on the shroud; 50~450 on the hub.
- **28 hours** with **32** CPUs to complete 20,000 iterations. (2.43 GHZ quad-core 64-bit Intel Xeon processor)

Computational domain in FLUENT

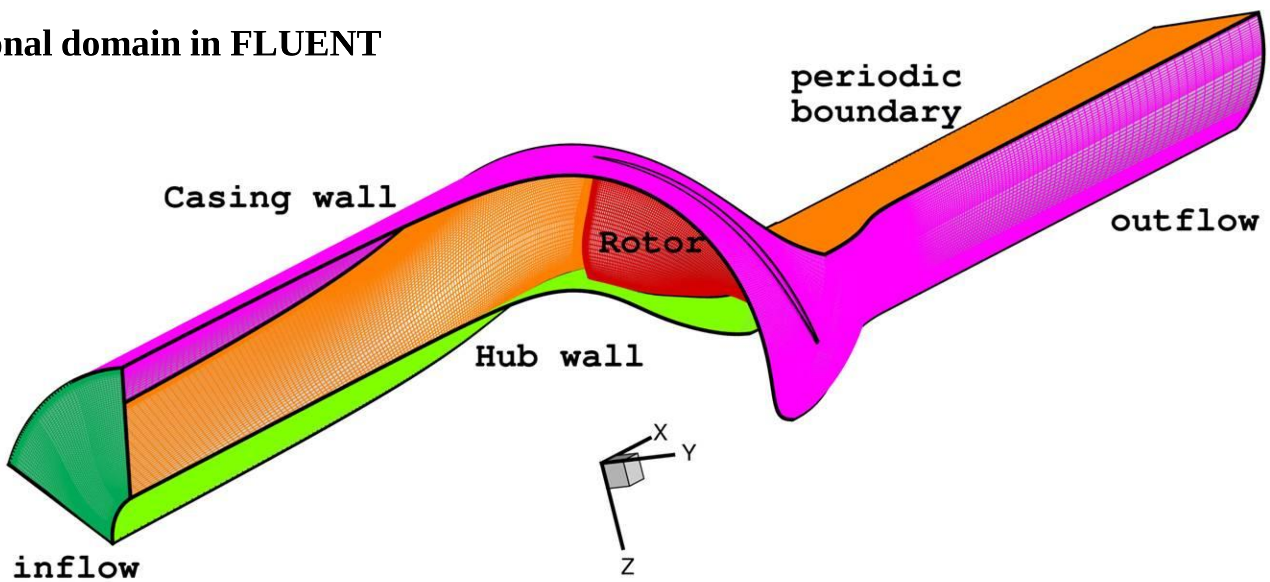

Numerical Results (Rotor Only)

- Comparison of -C_P (fully-wetted condition) on the rotor blade:

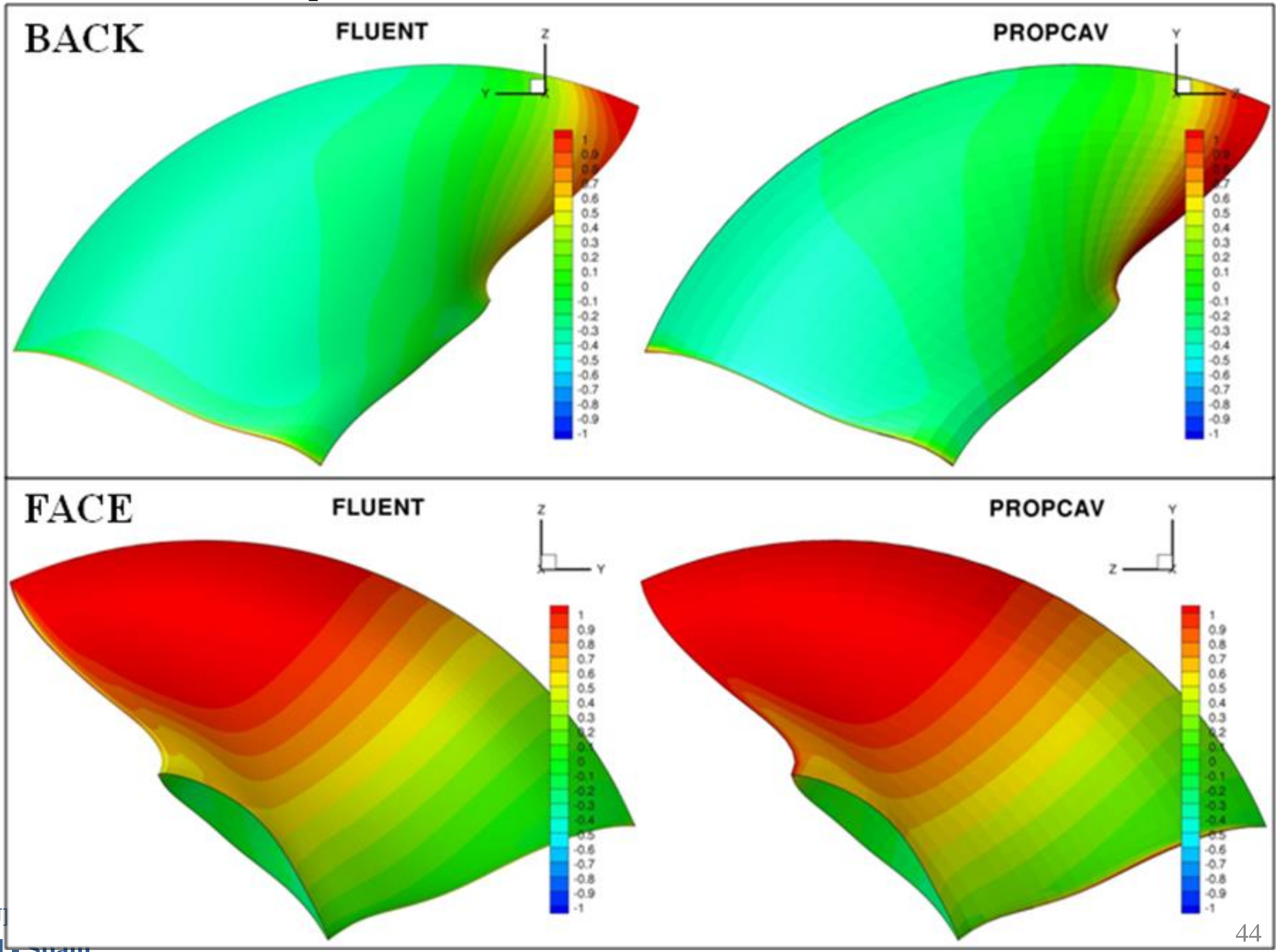

Numerical Results (Rotor Only fully-wetted simulation)

- Comparison of pressure distributions (**using C_f and viscous pitch correction**):

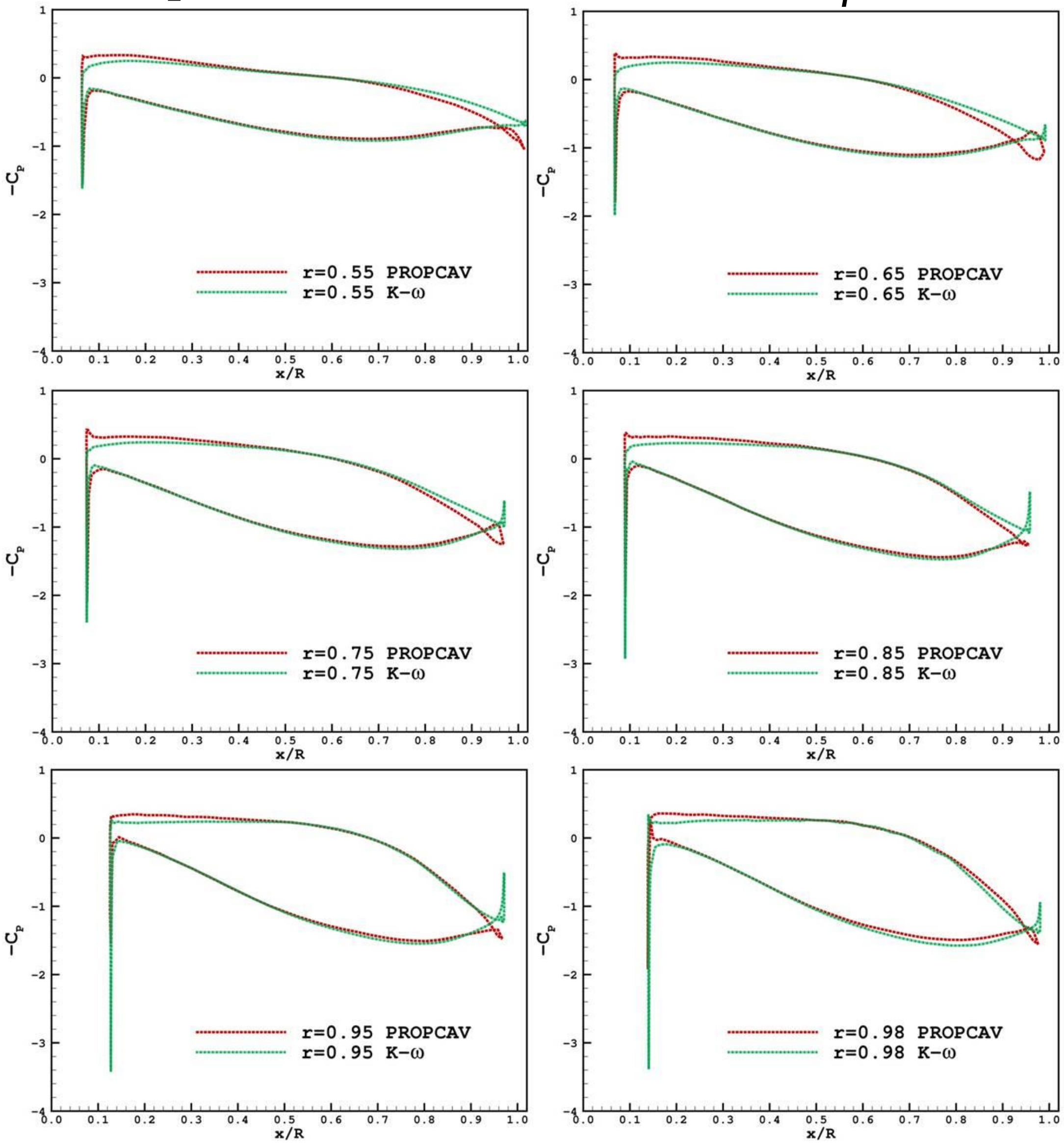

$$C_P = \frac{P - P_0}{0.5\rho n^2 D^2}$$

Numerical Results (Rotor Only fully-wetted simulation)

- Comparison of Power Coefficient (P^*)
  - Rotor only effect (**using C_f and viscous pitch correction**).

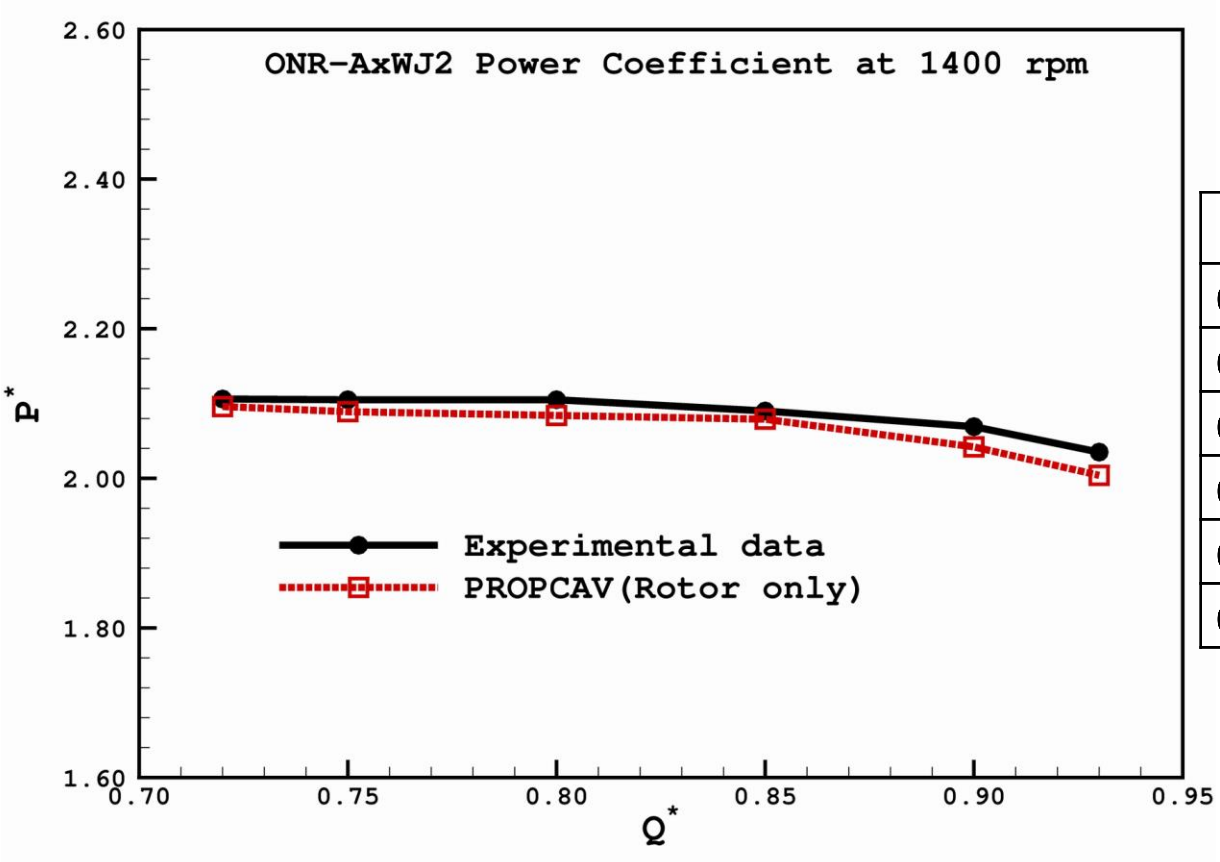

$$P^* = \frac{2\pi n Q}{\rho n^3 D^5} = 2\pi K_Q$$

Q^*	Experiment	PROPCAV	|Error| (%)
0.72	2.106	2.096	0.47
0.75	2.105	2.089	0.76
0.80	2.104	2.084	0.95
0.85	2.090	2.079	0.53
0.90	2.069	2.042	1.30
0.93	2.035	2.004	1.52

Numerical Results (Rotor Only fully-wetted simulation)

- Comparison of pressure distributions (**coupling with XFOIL**):

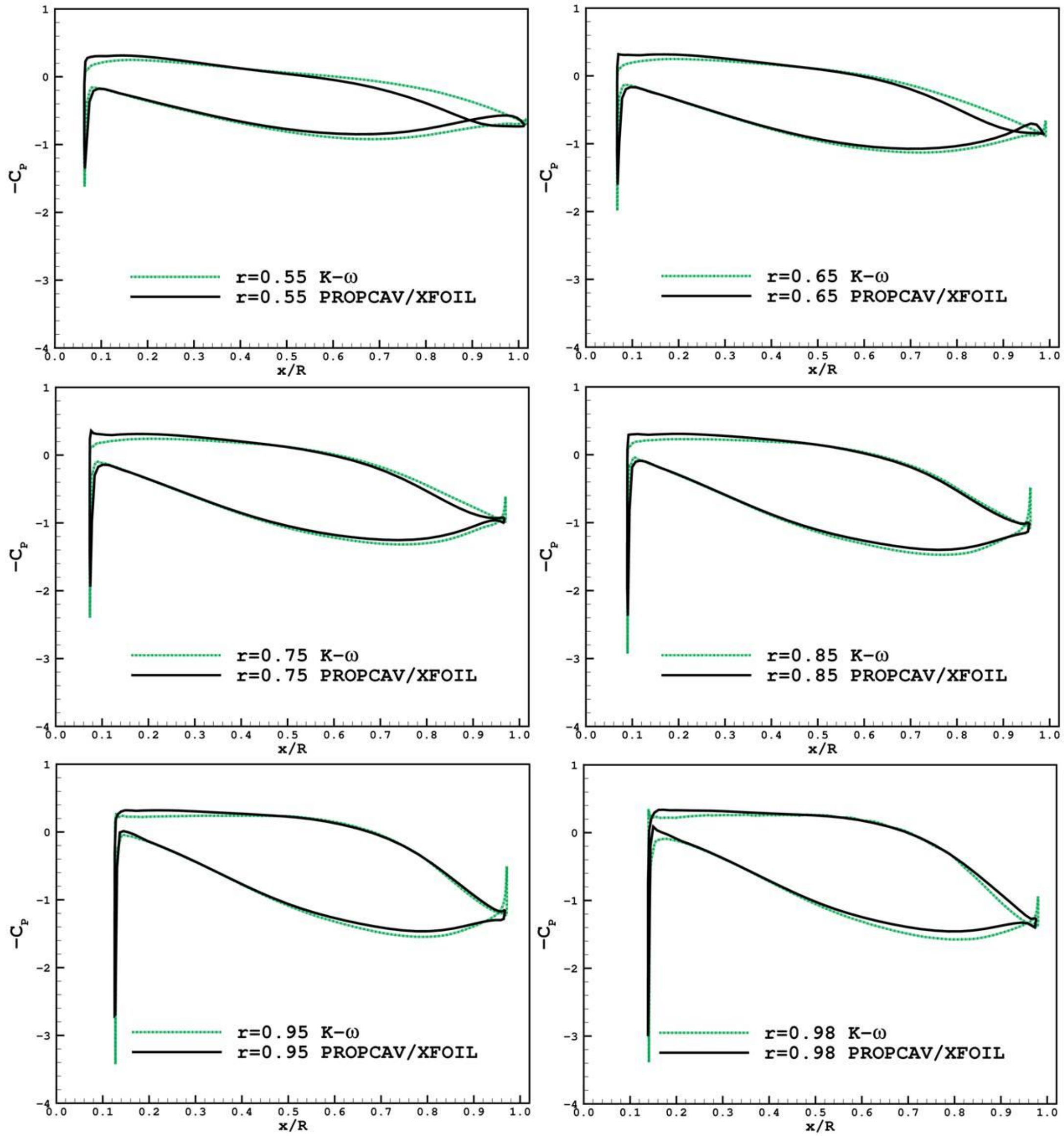

$$C_P = \frac{P - P_0}{0.5 \rho n^2 D^2}$$

- Comparison of the rotor blade geometry:

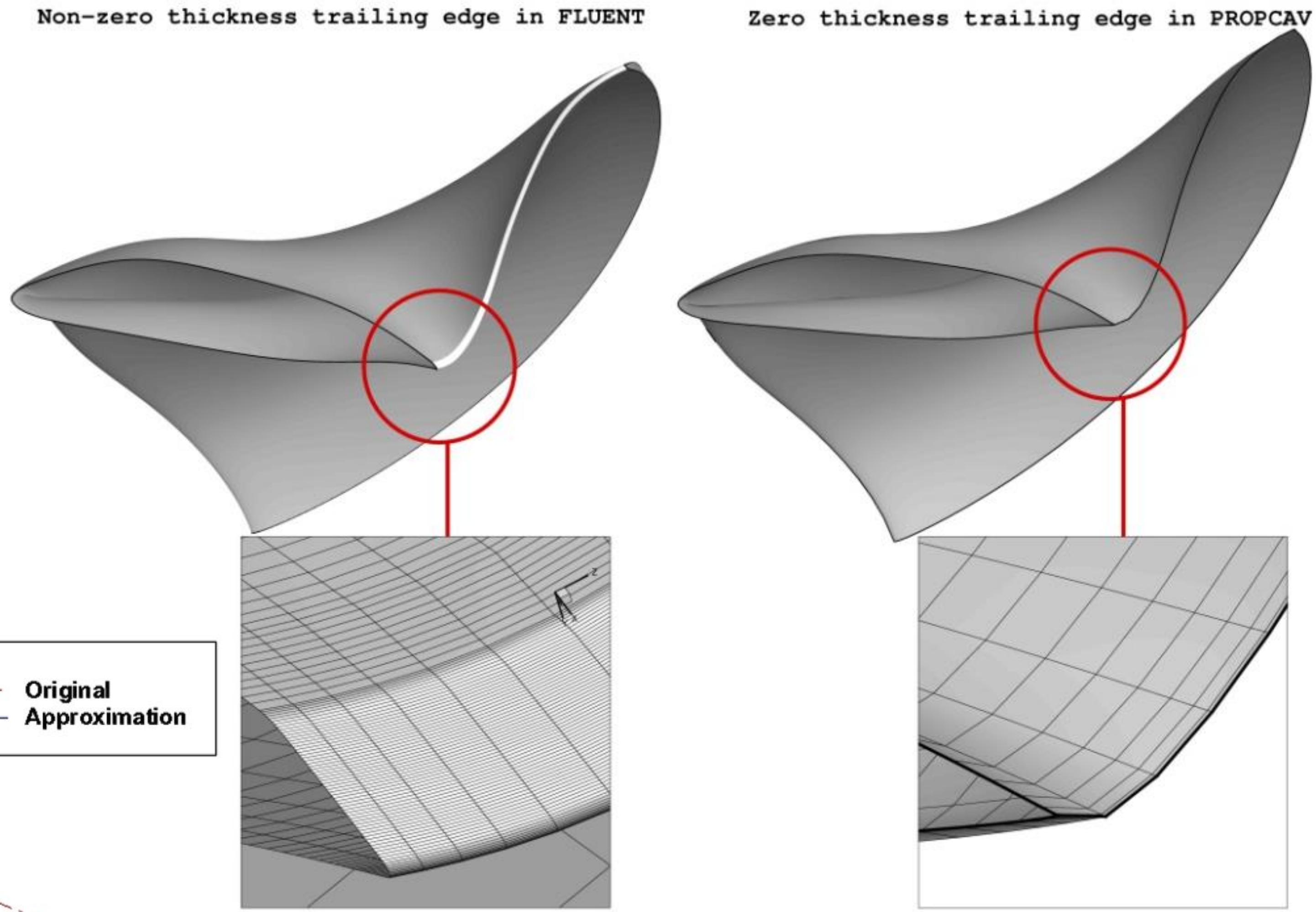

r/R=0.75

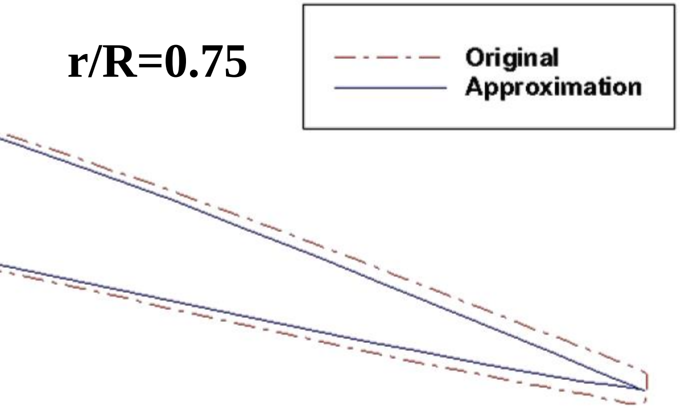

From Yu (MS/UT-OEG '12)

Alse see paper by Kinnas et al, SNH/ONR 2012 on a method which accounts some of the 3-D effects of boundary layer

Numerical Results (Rotor/Stator Interaction)

- Comparison of power coefficient (P^*) with experimental data and RANS:

$$P^* = \frac{2\pi n Q}{\rho n^3 D^5} = 2\pi K_Q$$

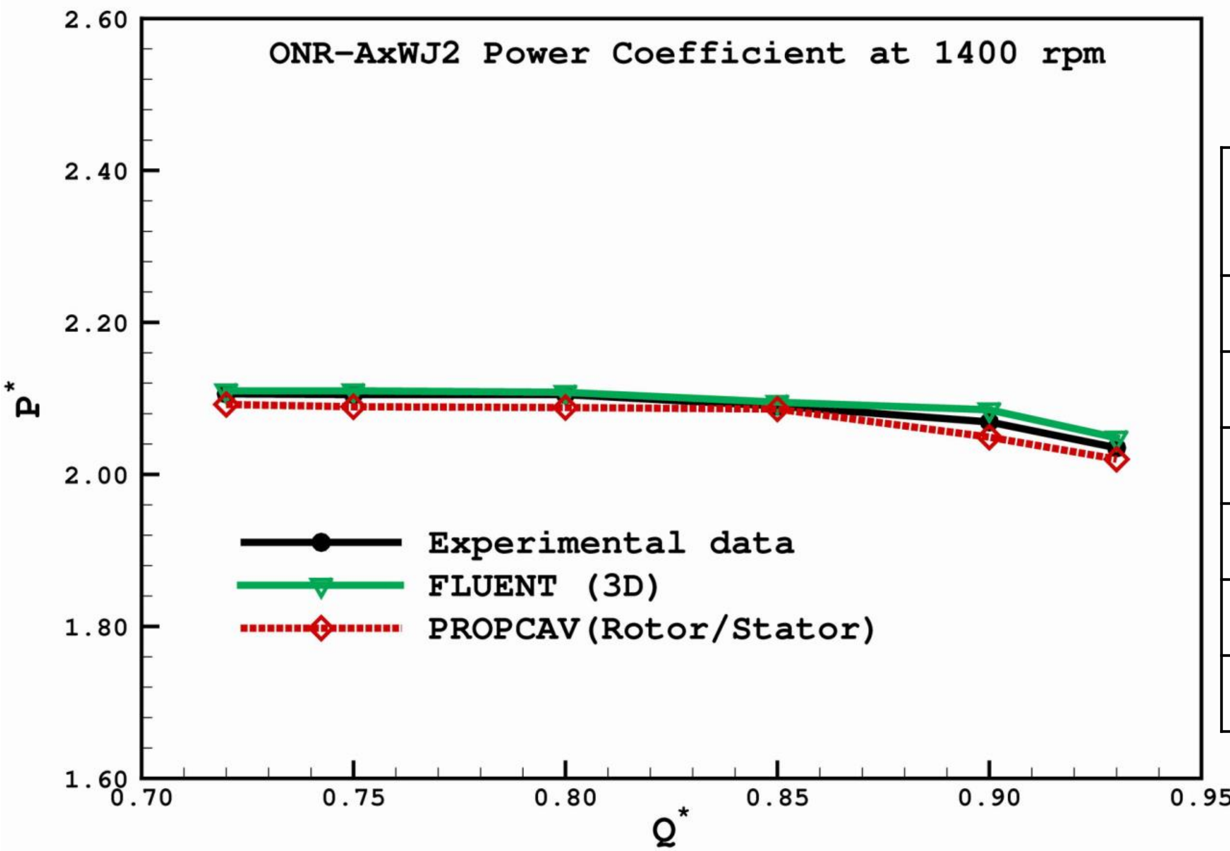

Q^*	Experiment	PROPCAV (RS Interaction)	|Error| (%)
0.72	2.106	2.092	0.66
0.75	2.105	2.089	0.76
0.80	2.104	2.088	0.79
0.85	2.090	2.086	0.19
0.90	2.069	2.049	0.97
0.93	2.035	2.020	0.74

Numerical Results (Rotor/Stator Interaction)

- Comparison of pressure head (***H****) on the shroud with experimental data and RANS:

$$H^* = \frac{P_{t6} - P_{t3}}{\rho n^2 D^2}$$

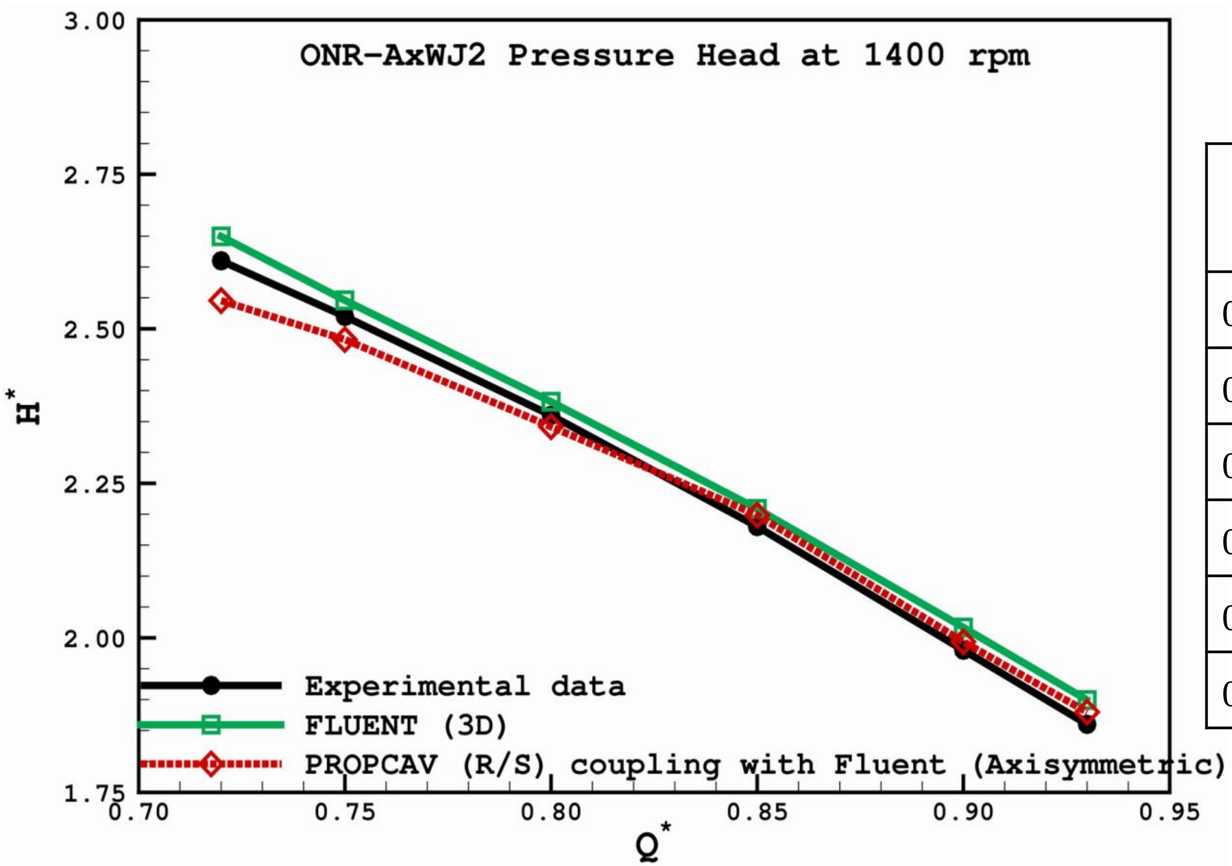

Q^*	Experiment	PROPCAV (RS Interaction)	|Error| (%)
0.72	2.61	2.55	2.30
0.75	2.52	2.48	1.59
0.80	2.36	2.34	0.85
0.85	2.18	2.20	0.92
0.90	1.98	1.99	0.51
0.93	1.86	1.88	1.08

Numerical Results (Rotor/Stator Interaction)

- Comparison of predicted efficiency (η):

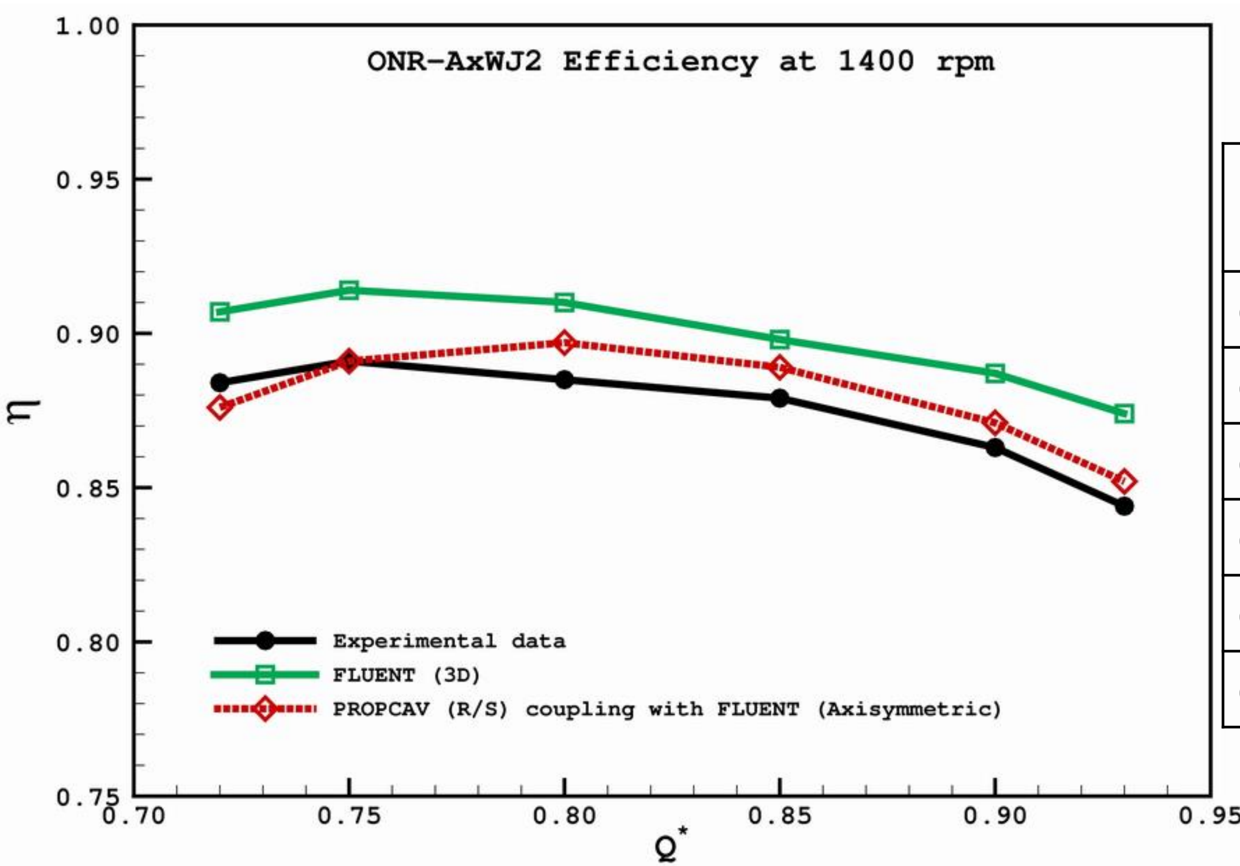

$$\eta = \frac{Q^* H^*}{P^*}, \; and \; Q^* = \frac{Q_J}{nD^3}$$

Q^*	Experiment	PROPCAV (RS Interaction)	|Error| (%)
0.72	0.884	0.876	0.90
0.75	0.891	0.891	0.00
0.80	0.885	0.897	1.36
0.85	0.879	0.889	1.14
0.90	0.863	0.871	0.93
0.93	0.844	0.852	0.95

Numerical Results (Cavitating)

- Rotor Cavitation Coverage

Experiments and
CFX simulations by
Chesnakas et al. (2009)

Convergence and grid
dependence studies may be
found in Chang & Kinnas
(CAV ′12; SNH ′12) and
Chang (PhD/UT-OEG ′12)

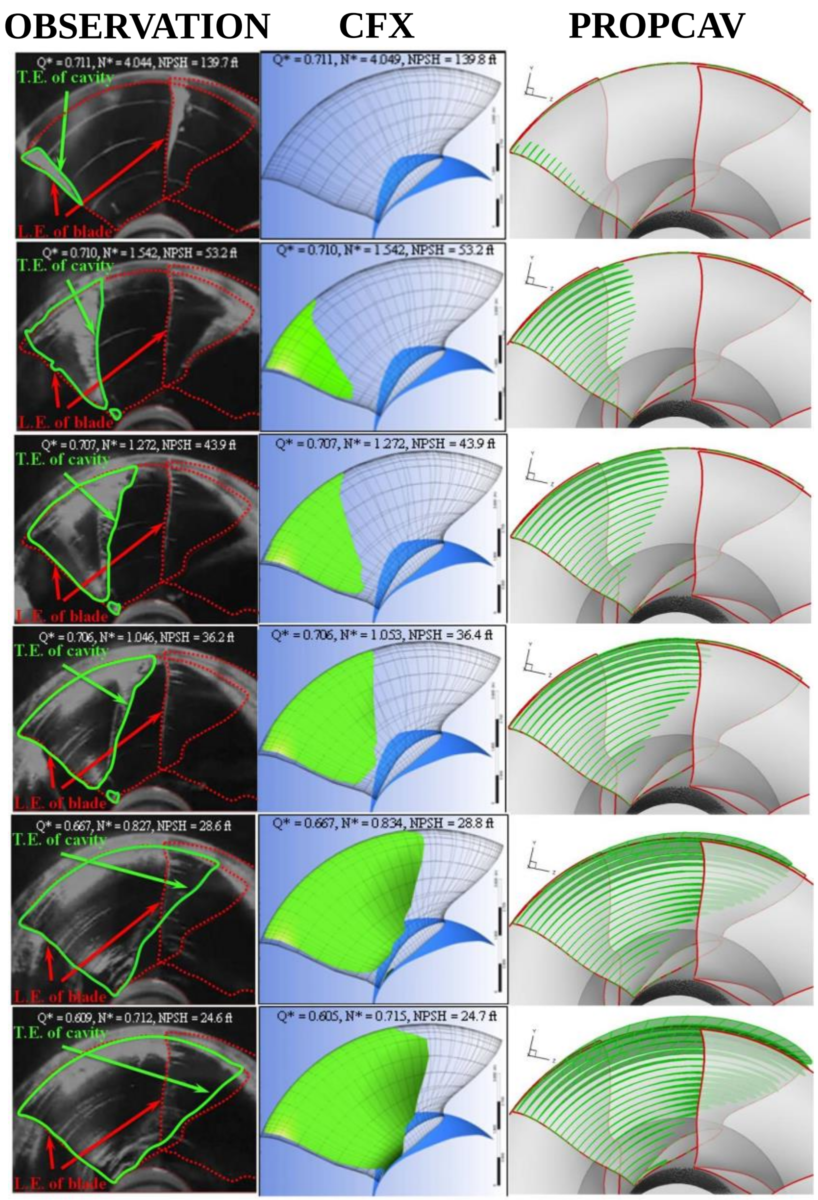

Numerical Results (Thrust and Torque Breakdown)

- Cavity patterns on the rotor blade (at ***Q****=0.830 and ***N****=0.993).

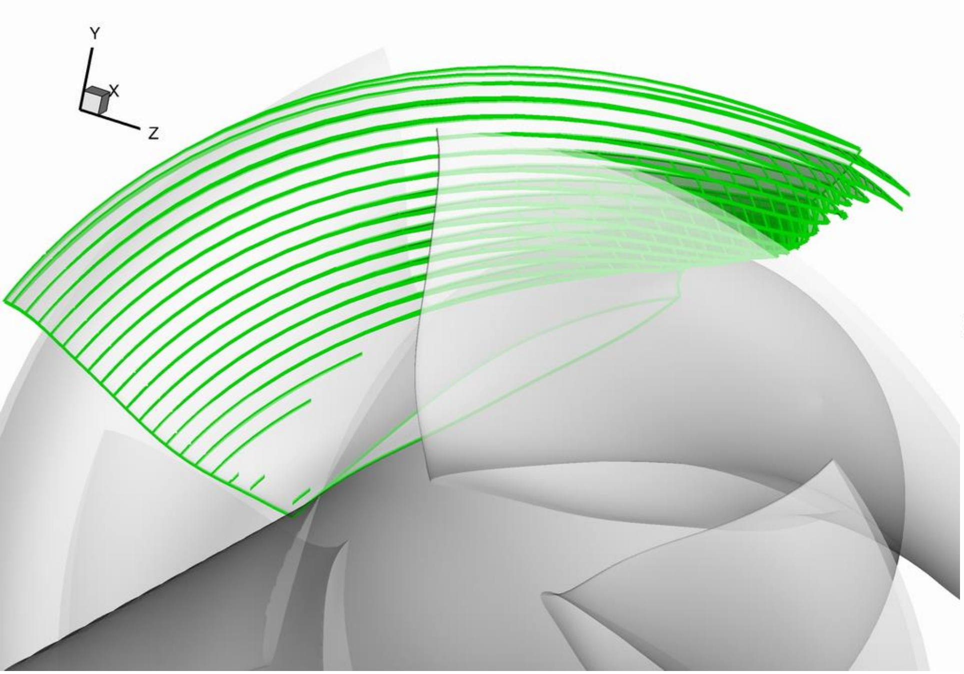

- Pressure distributions on the rotor at ***r/R***=0.988. Comparison between fully-wetted and cavitating solutions (at ***Q****=0.830 and ***N****=0.993).

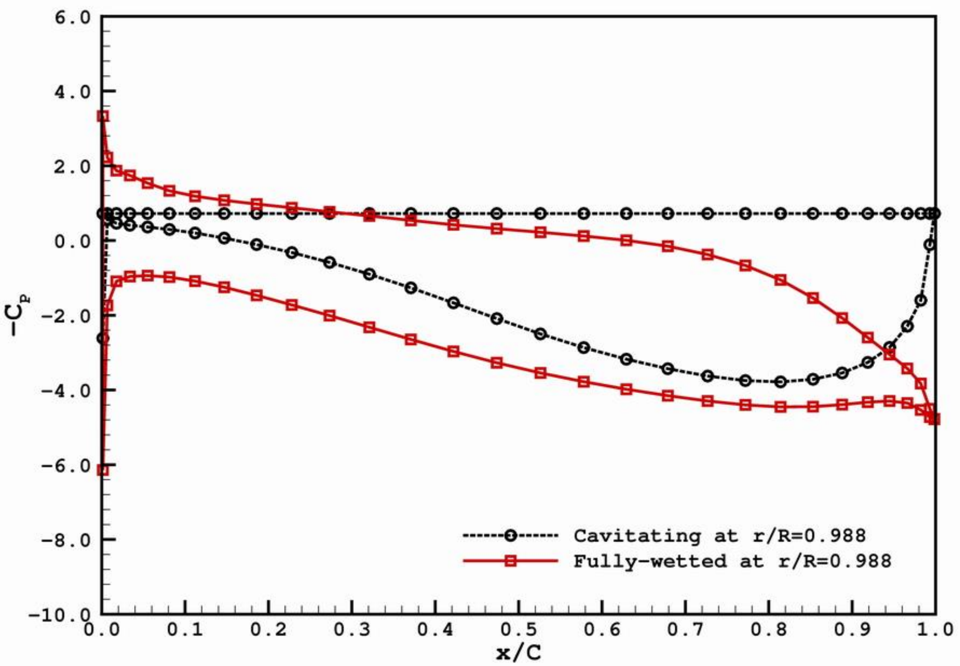

Numerical Results (Thrust and Torque Breakdown)

- Comparison of wetted and cavitating circulation distributions (at Q^*=0.83 and N^*=0.993):

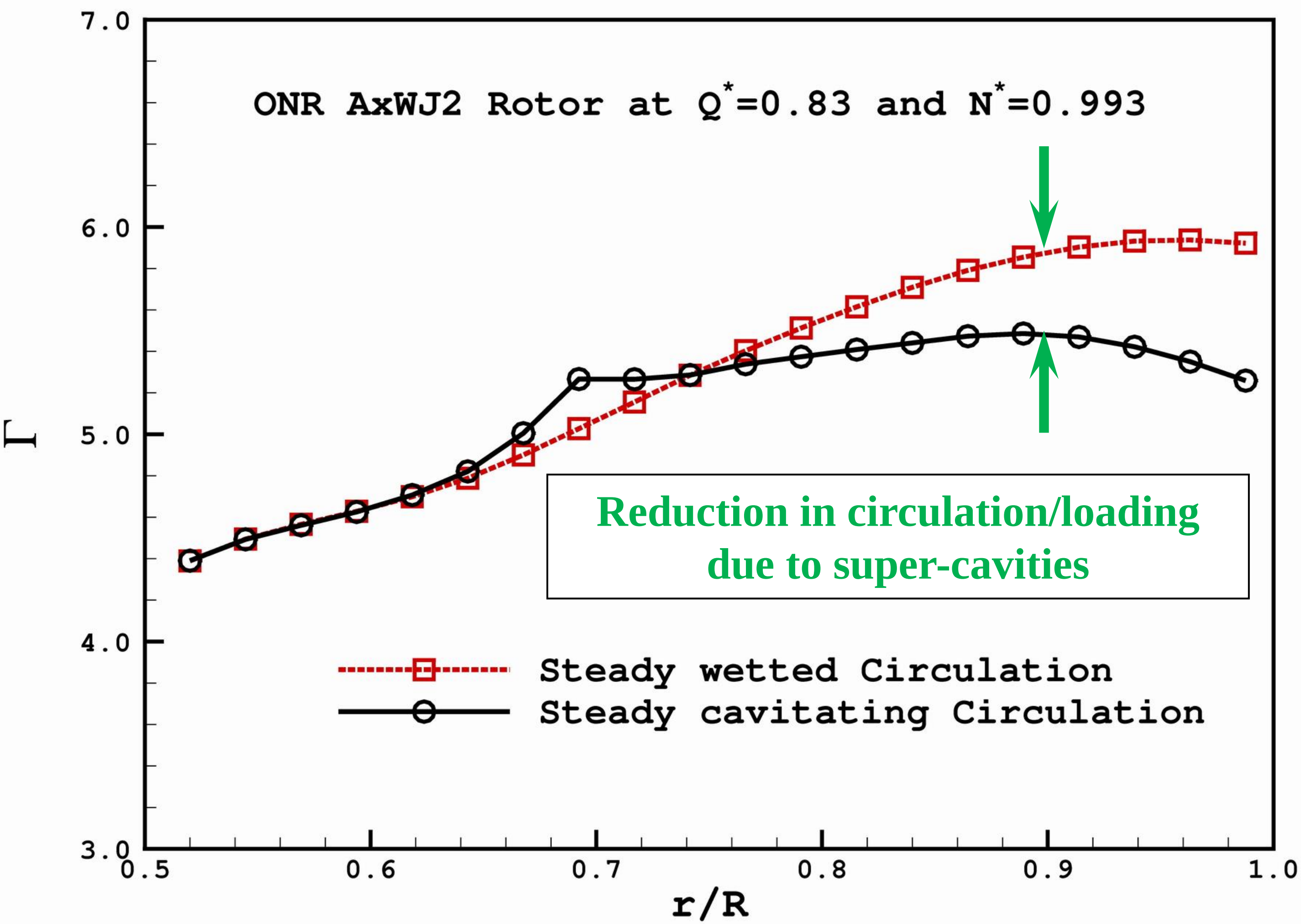

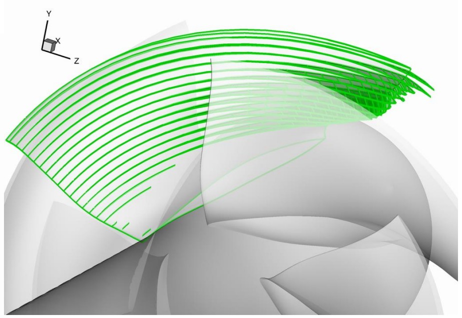

Numerical Results (Thrust and Torque Breakdown)

- Comparison of the predicted rotor normalized **thrust** (using non-cavitating thrust at ***Q****=0.83) with experimental data for various flow coefficients (***N****).
- Comparison of the predicted rotor normalized **torque** (using non-cavitating torque at ***Q****=0.83) with experimental data for various flow coefficients (***N****).

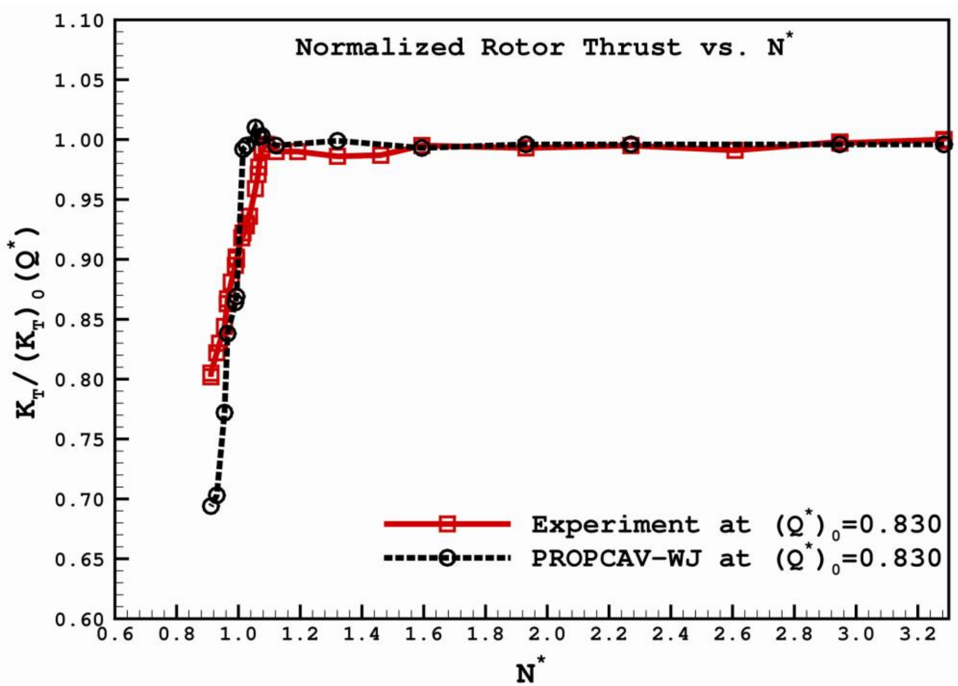

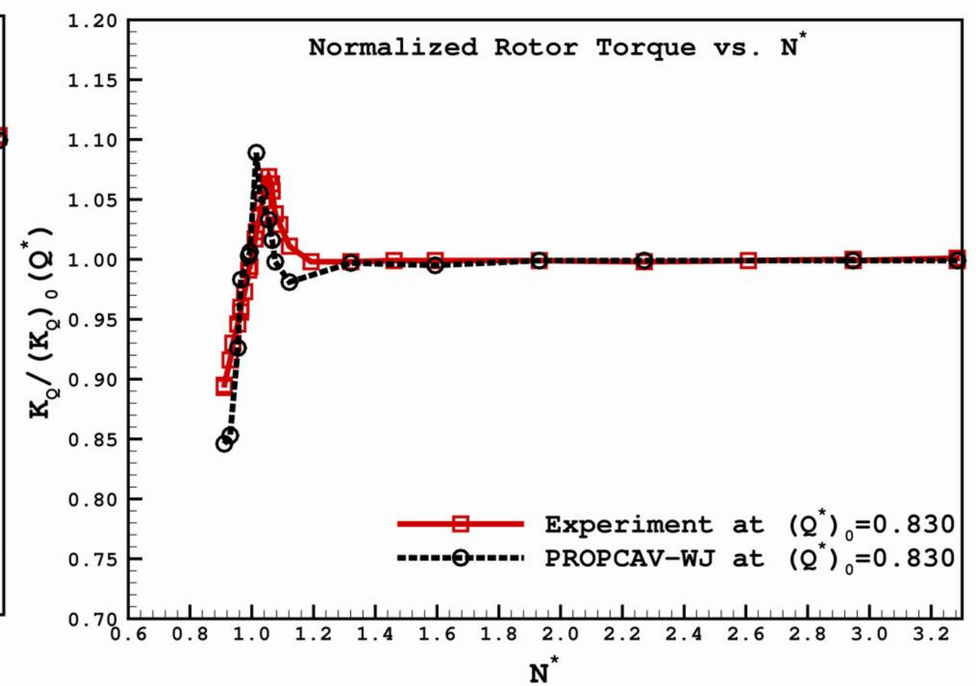

Design Methods

Propeller Blade Design (what is given)

- Ship speed, V_s , RPS n, Propeller radius R
- Inflow distribution $V(r,\theta)$ at the propeller plane (nominal wake) in the absence of the propeller; usually measured in model tests (EFD) or computed via CFD. Must determine effective wake (= nominal wake-propeller induced flow) via coupling of inflow with MPUF-3A or PROPCAV.
- The required thrust T (based on hull resistance in the absence of the propeller) to be provided by the propeller. The hull resistance must be adjusted (increased) to account for interaction with propeller (integrated prop/hull design)

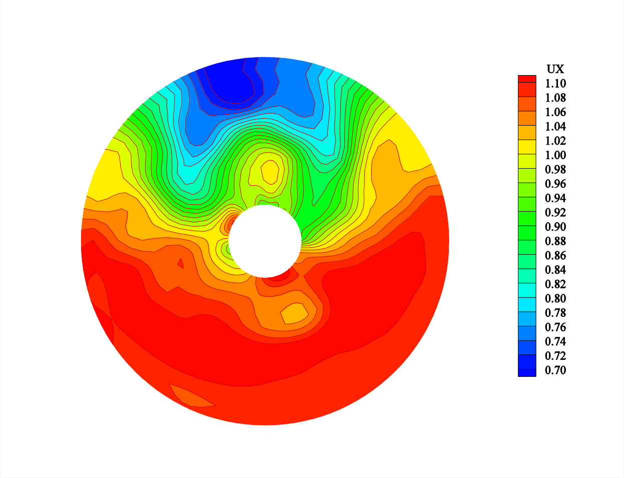

Propeller Blade Design (what we wish)

- We wish to design the <u>most efficient propeller</u> (i.e. requires minimum power P or minimal torque Q for fixed RPS, n) AND exhibits none or minimal (acceptable) amount of cavitation and produces related <u>minimal (acceptable) hull pressure fluctuations</u>, and emitted noise.

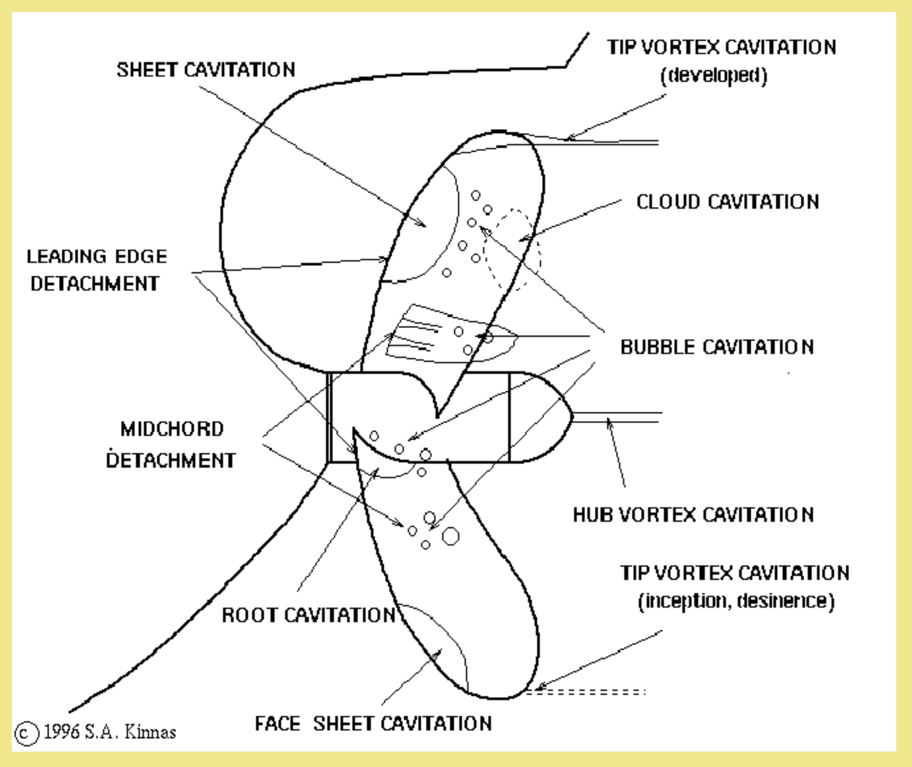

Propeller Blade Design (what is fixed)

- Chord-wise blade thickness distribution (τ/τ_{max} vs. x/c) is chosen so that it allows for maximum range of angles of attack (+/-AOA) for cavitation free operation (usually modified NACA-66 section)
- Chord-wise blade camber distribution (f/f_{max} vs. x/c) is usually NACA a=0.8 mean-line or has a loading distribution (Δp vs. x/c) which is the same as that of NACA a=0.8 distribution
- Distribution of max thickness (τ_{max}/D vs. r/R) in the radial direction is given based on structural criteria. Detailed structural analysis (after the blade has been designed) can check/modify τ_{max}, and redo design.
- Skew/rake of the blade is chosen based on information on the variation of the inflow in the circumferential direction

Propeller Blade Design (what is to be determined)

- Chord distribution (c/D vs. r/R) in the radial direction, based on the selected thickness distribution and τ_{max}/D and the cavitation number ($\sigma_n = p_{shaft} - p_v / \rho n^2 D^2$), for cavitation free operation
- Pitch distribution (P/D vs. r/R)
- Camber distribution f/c vs. x/c at all radial locations (r/R) or f_{max}/D vs. r/R

Propeller Blade Design (trends)

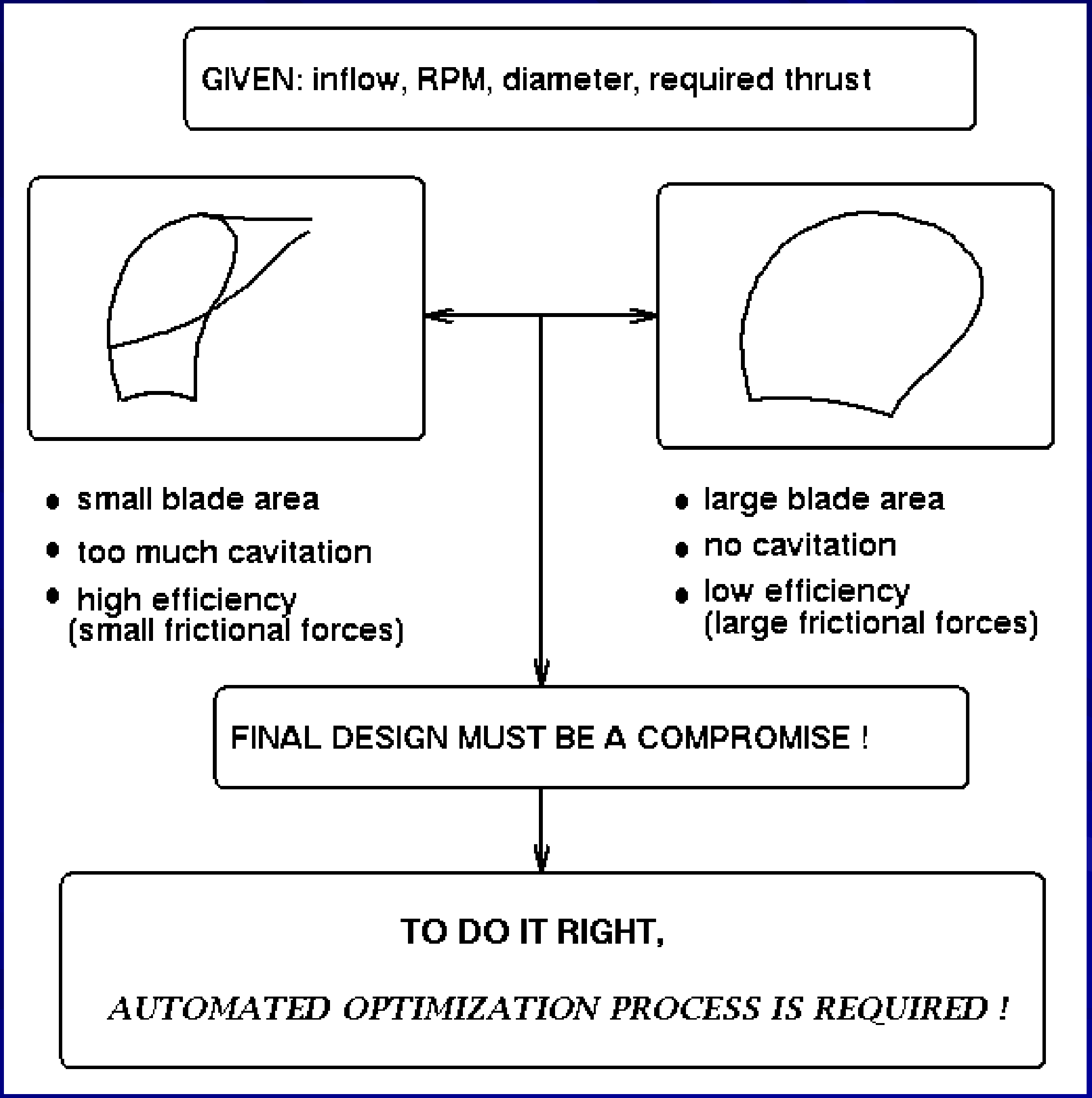

Propeller Blade Design (approaches)

- Traditional philosophy: Determine optimum circulation distribution in **circumferentially averaged inflow (using a lifting line model)**, design blade to develop optimum circulation, analyze design in actual inflow, and then adjust accordingly (**trial & error**) based on predicted cavitation
- Our philosophy: Design blade via optimization techniques in the **actual inflow** (CAVOPT-3D: B-spline blade description combined with 2^{nd} order Taylor expansions of the objective function in the vicinity of the solution, Mishima PhD, '96, Mishima and Kinnas, JSR'97, Griffin and Kinnas, JFE'98)

CAVOPT-3D

(blade described via 13-16 B-spline parameters)

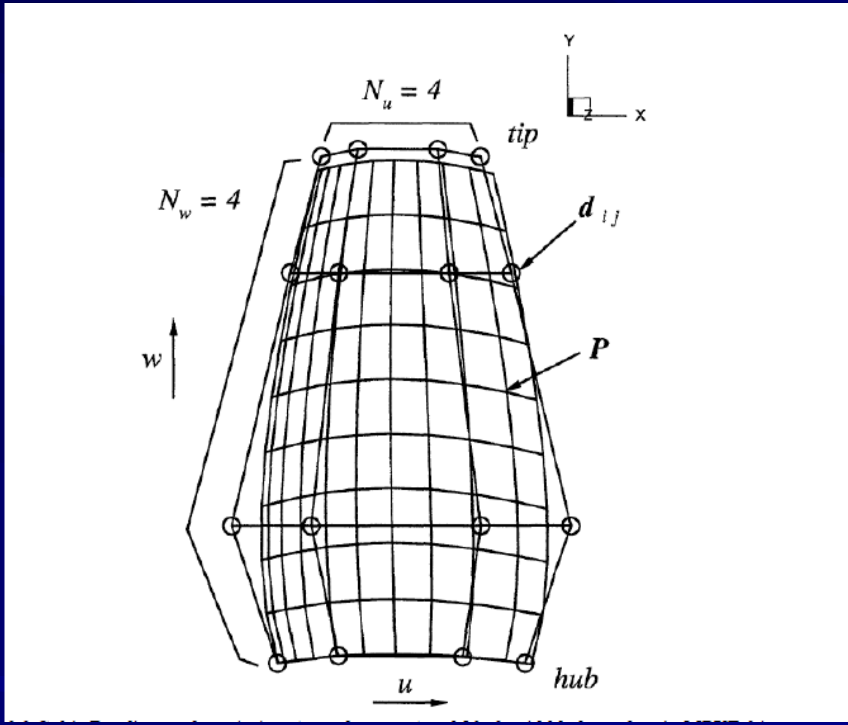

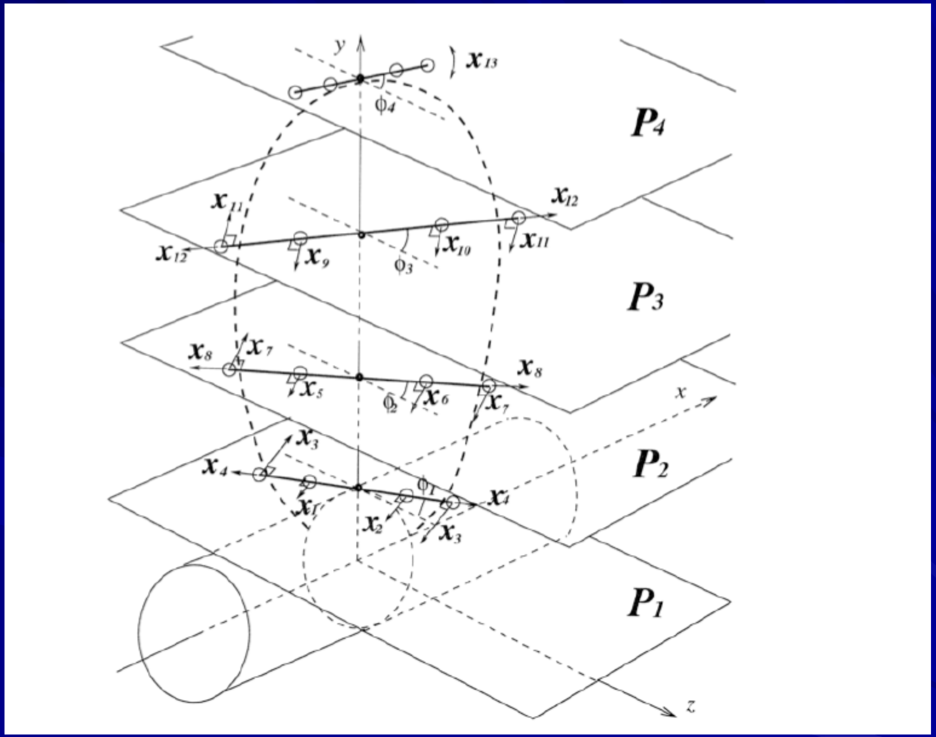

MPUF-3A is running <u>within</u> CAVOPT-3D until convergence (usually takes about 500 runs, depending on tolerance)

CAVOPT-BASE

(Kinnas et al, SNAME Trans. 2005, Deng, MS/OEG-UT 2005)

- Propeller family generation

$$(P/D)_{design} = x_1 * (P/D)_{base}$$

$$(c/D)_{design} = x_2 * (c/D)_{base}$$

$$(f/c)_{design} = x_3 * (f/c)_{base}$$

x_1, x_2,x_3 are the design variables.

- Performance database (**created by running MPUF-3A over several combinations of x1, x2, x3, e.g. 10x10x10 runs**)

Propeller performances					Design variables		
KT	KQ	CA	Cpmin	……	x1	x2	x3

Database Approximation

Express the propeller performances, KT, KQ, CA, C_{Pmin} as functions of the design variables.

$$K_T = \frac{T}{\rho n^2 D^4} = f_1(x_1, x_2, x_3)$$

$$K_Q = \frac{T}{\rho n^2 D^5} = f_2(x_1, x_2, x_3)$$

$$CA = \frac{Cavity.Area}{Blade.Area} = f_3(x_1, x_2, x_3)$$

$$C_{p\min} = \frac{p - p_{shaft}}{\rho n^2 D^2} = f_4(x_1, x_2, x_3)$$

The expressions of $f_1, \ldots, f_4$ are approximated by the Least Square Method (LSM) or the linear interpolation method (LINTP)

Database Approximation (previous approach)

- Least Squares Method (LSM)

Example : 2nd order polynomial

$$f_i(x_1, x_2, x_3) = a_{i,1}x_1^2 + a_{i,2}x_2^2 + a_{i,3}x_3^2$$
$$+a_{i,4}x_1x_2 + a_{i,5}x_2x_3 + a_{i,6}x_1x_3$$
$$+a_{i,7}x_1 + a_{i,8}x_2 + a_{i,9}x_3$$
$$+a_{i,10} \qquad i = 1,\ldots,4$$

The coefficients are determined to minimize RMS errors.

Database Approximation (new approach)

- Linear Interpolation Method (LINTP) within each cell of the database

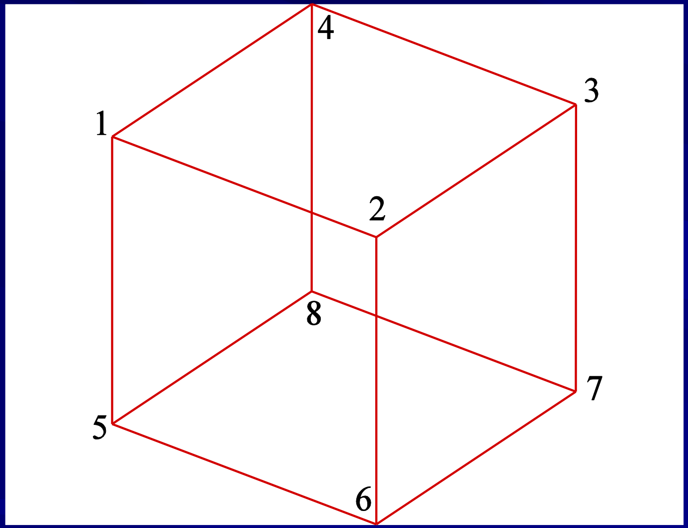

The function value of the point, (x_1,x_2,x_3) inside the cell is:

$$
\begin{aligned}
f(x_1, x_2, x_3) = {} & a_1 x_1 x_2 x_3 \\
& + a_2 x_1 x_2 + a_3 x_2 x_3 + a_4 x_1 x_3 \\
& + a_5 x_1 + a_6 x_2 + a_7 x_3 \\
& + a_8
\end{aligned}
$$

The coefficients, a_i, $i = 1, 2, \ldots, 8$, are determined from the values at eight vertices.

Optimization Problem

Minimize $K_Q\,(x)$

Subject to $K_T\left(x\right) = KTo$

$CA(x) \leq CAMAX$

Cavitating case

min [p(x,y,z;t)] > p_{vapor} $-\,C_{P\min}\,(x) \leq CPMIN$

Fully wetted case

$x_1^{\min} \leq x_1 \leq x_1^{\max}$

$x_2^{\min} \leq x_2 \leq x_2^{\max}$

$x_3^{\min} \leq x_3 \leq x_3^{\max}$

CPMIN=σ_n-TOL

The constrained nonlinear optimization is solved by **augmented Lagrangian penalty method** (Mishima & Kinnas, 1996).

CAVOPT-BASE/Sample cases

- No. 1: Wetted open propeller subject to uniform inflow
- No. 1a: Wetted open propeller subject to non-axisymmetric inflow
- No. 1b: Cavitating open propeller subject to non-axisymmetric inflow
- No. 2: Fully wetted ducted propeller subject to uniform inflow
- No. 2a: Fully wetted ducted propeller subject to non-axisymmetric inflow
- No. 3: Cavitating propeller inside tunnel subject to non-axisymmetric inflow

NOTE: Only results from case 3 will be shown in the nest slides.

Design case No. 3

- **Cavitating propeller inside tunnel subject to non-axisymmetric inflow**
  - N3745 Propeller
  - Design conditions

$\sigma = 3.0,\ \ F_n = 5.0$

$J_s = 0.95,\ \ K_{Ttotal} = 0.4$

$CA \le 30\%,\ \ C_f = 0.004$

Domain of design variables

$$0.8 \le x_1 \le 1.2$$

$$0.6 \le x_2 \le 1.2$$

$$0.0 \le x_3 \le 3.0$$

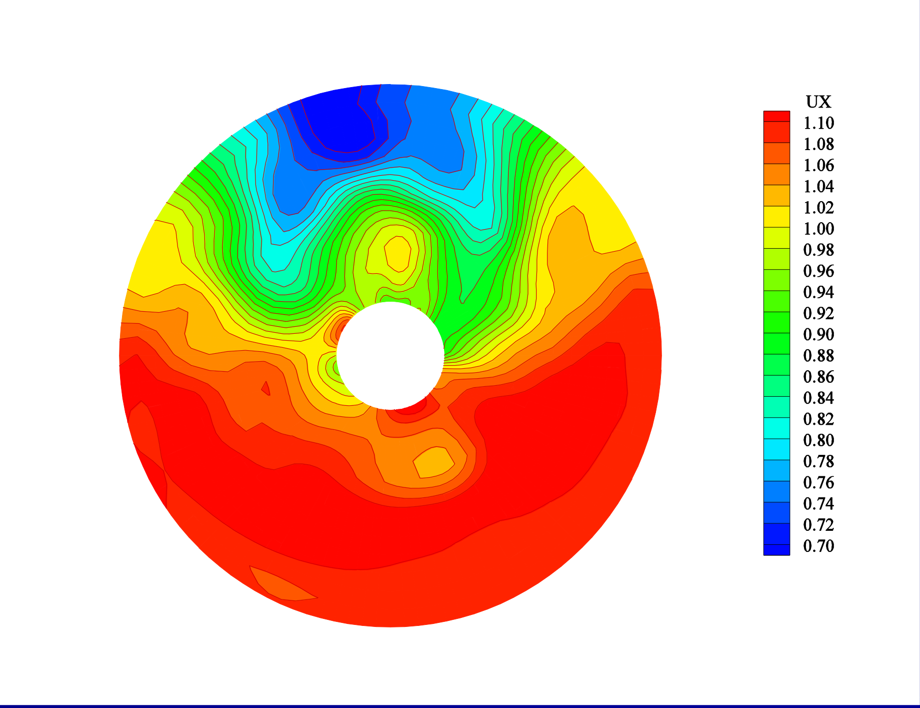

Nominal wake

Design case No. 3

- Cavitating propeller inside tunnel subject to non-axisymmetric inflow
  - Optimal solutions and design results

	$X_{1\text{-}OPT}$	$X_{2\text{-}OPT}$	$X_{3\text{-}OPT}$
Present method (CAVOPT-BASE)	0.8728	0.9566	1.3333

	KT	**10KQ**	**Efficiency**	**CA**
Present method (CAVOPT-BASE)	0.3977	0.7903	76.1%	30.2%

Design case No. 3

- Cavitating propeller inside tunnel subject to non-axisymmetric inflow

Cavity constraints	Optimal solutions			Design results			
	x_1	x_2	x_3	KT	10KQ	Eff	CA
5%	0.8149	1.2000	2.1904	0.4014	0.8737	69.5%	5.0%
10%	0.8448	1.2000	1.6785	0.3999	0.8245	73.3%	10.0%
20%	0.8542	1.0000	1.6185	0.4015	0.8051	75.4%	19.3%
30%	0.8728	0.9566	1.3333	0.3977	0.7903	76.1%	30.2%
40%	0.8742	0.9333	1.3333	0.3954	0.7851	76.1%	32.1%

Effect of max allowed cavity area on blade shape/efficiency

Design case No. 3: Effect of Max. Allowed cavity extent on efficiency of optimum blade

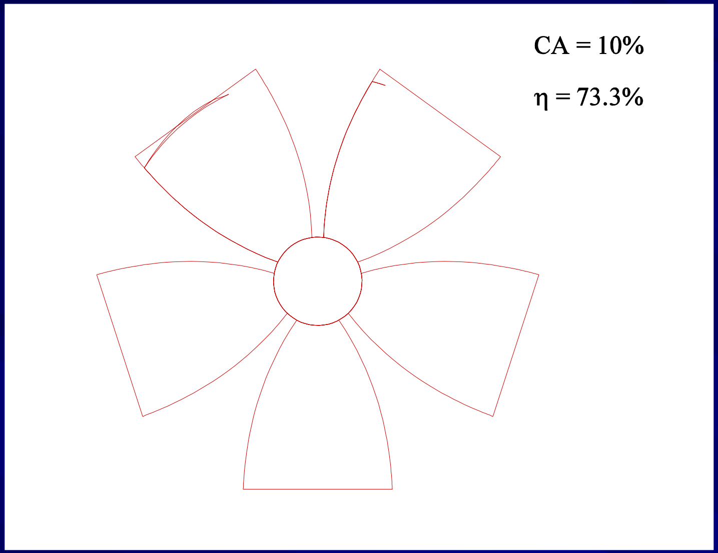

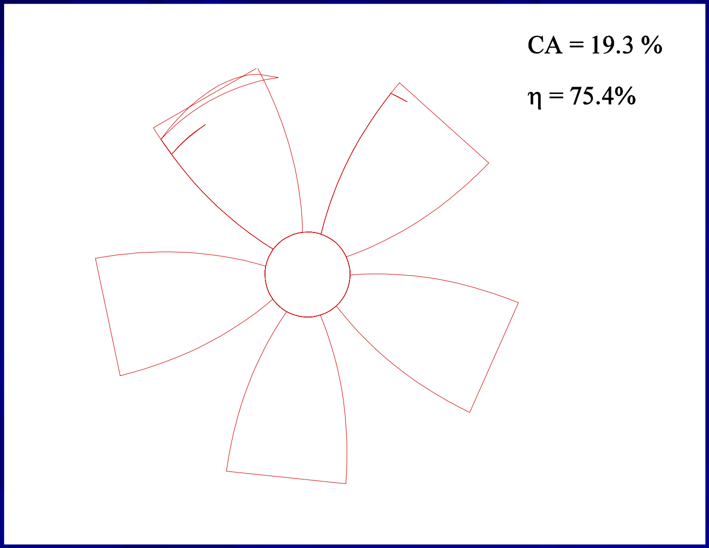

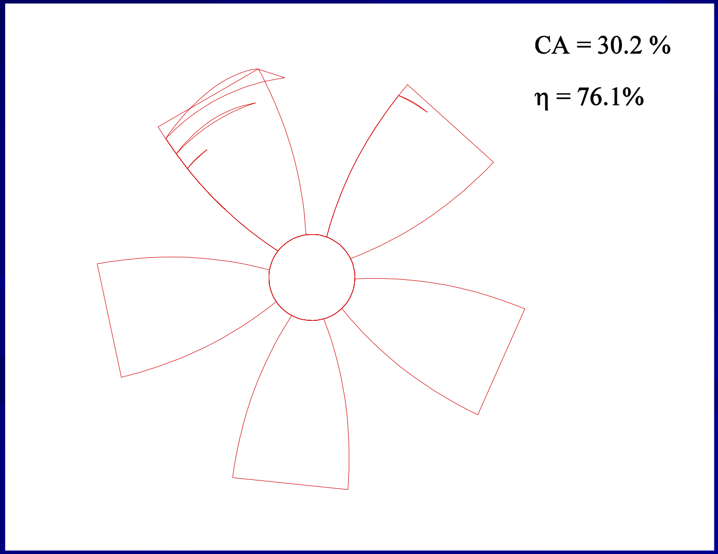

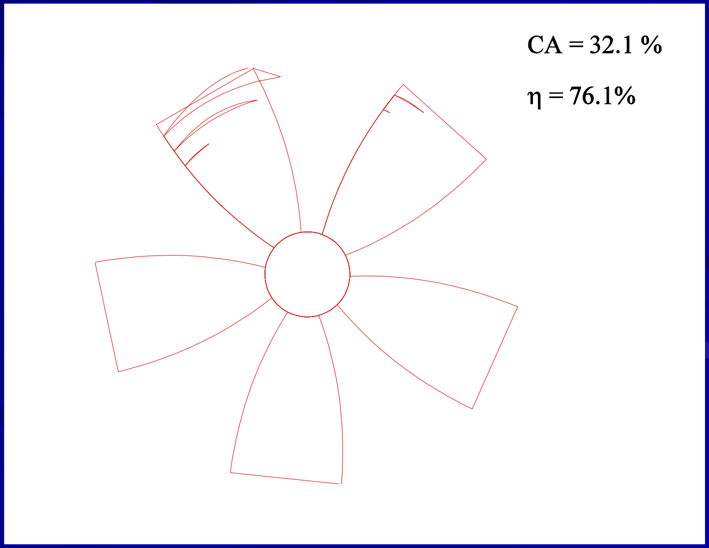

Design case No. 3

- Cavitating propeller inside tunnel subject to non-axisymmetric inflow

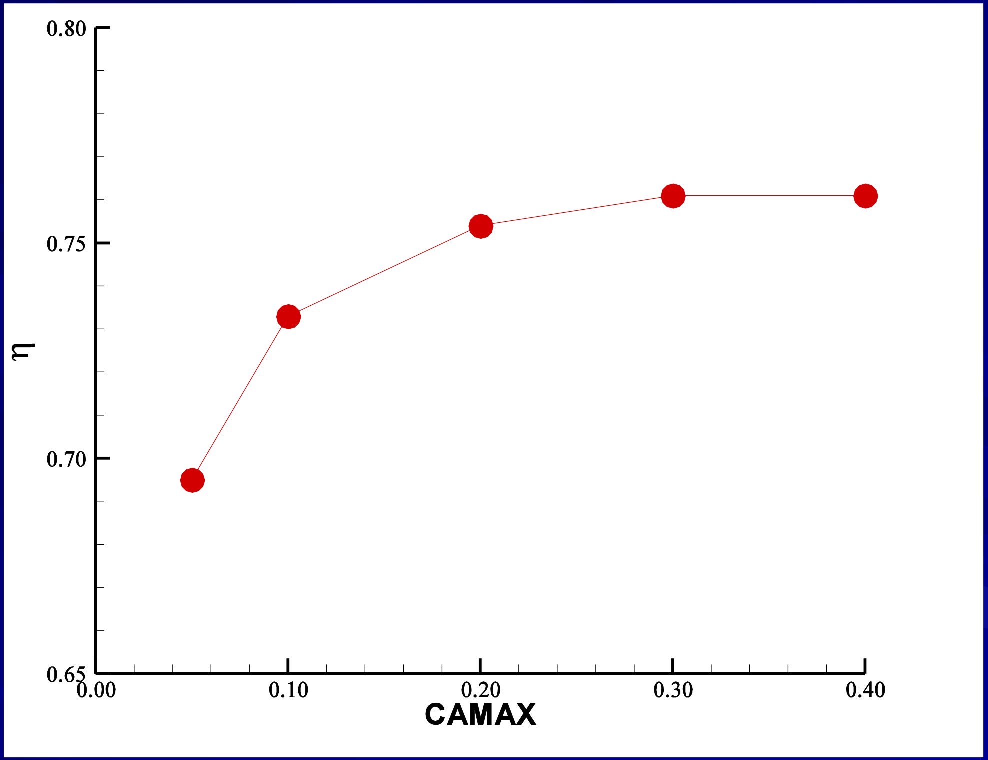

Effect of max allowed cavity area on propeller efficiency

Other models

- They involve application of RANS, LES, DES, DNS, and two-phase models for sheet or other types of cavitation (including cloud) (e.g. work of Prof. Abdel-Maksoud at Tech. Univ. of Hamburg, or Prof. Carrica at the Univ. of Iowa)
- LES seems to be more proper for propeller crash-back conditions, when the propeller reverses for the ship to stop (e.g. see work of Prof. Mahesh at the Univ. of Minnesota)
- Recent efforts include interaction with material properties for the prediction of cavitation erosion (e.g. see work Drs. Chahine and J-K Choi at Dynaflow)

Some of our most recent efforts include:

- An new model (VISVE) based on solving the VIScous Vorticity Equation in 3-D and coupling with PROPCAV (PhD of Ye Tian, OEG 2014, Tian & Kinnas, SNH/ONR 2014)

- Application of MPU-3A/RANS to two blade row flows (in the past we had done the same where we used Euler instead of RANS)

Results from VISVE/PROPCAV

- **A propeller at low Advance Ratio J=0.3**

Grid is only placed close to the blade where the vorticity is expected not to be zero

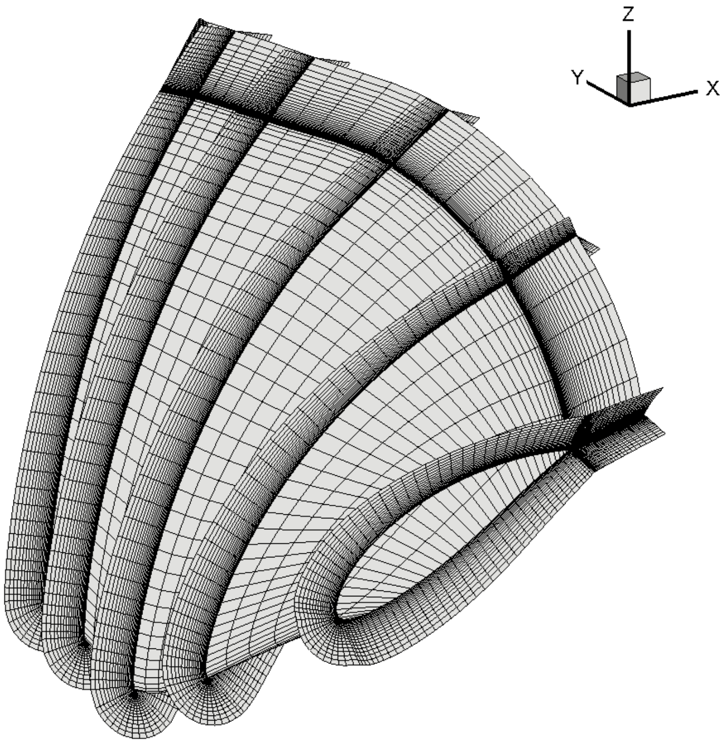

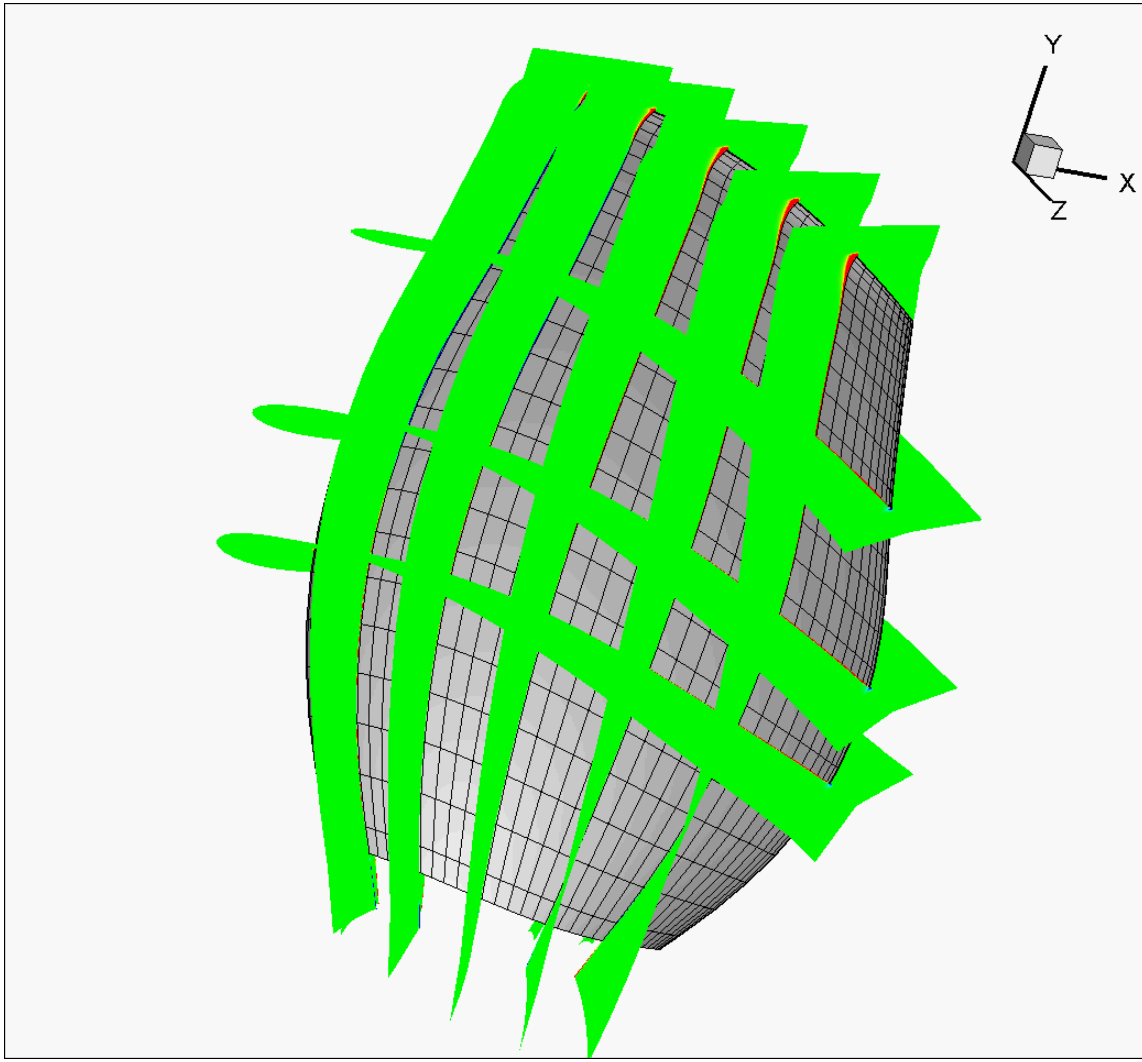

- **Application of MPU-3A/RANS to two Contra-rotating blade row flows for an azimuthal thruster**

MPUF-3A grid for downstream propeller

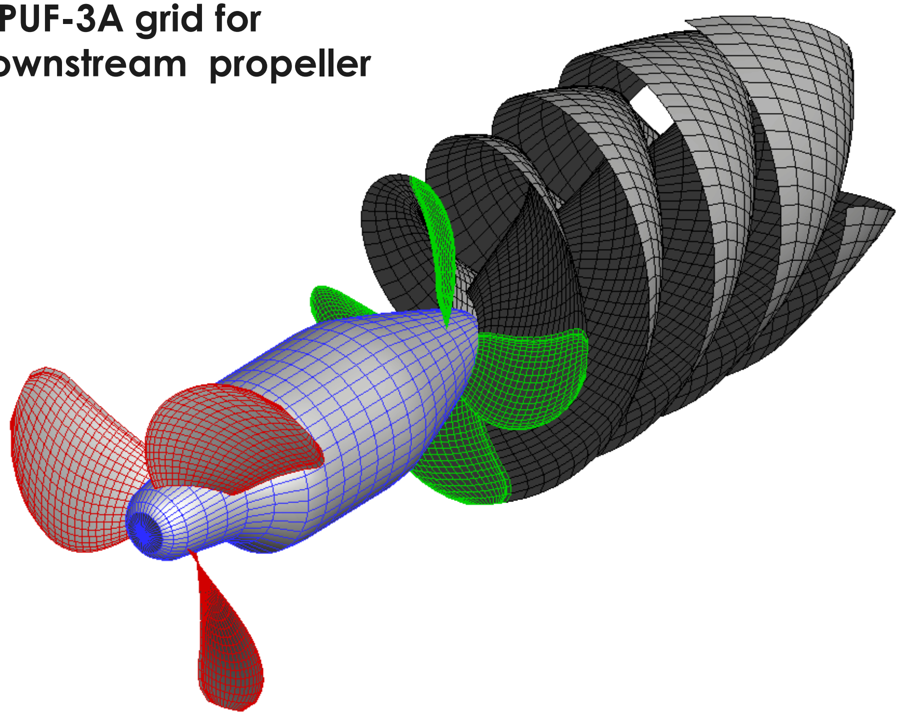

Propellers represented with body forces in RANS

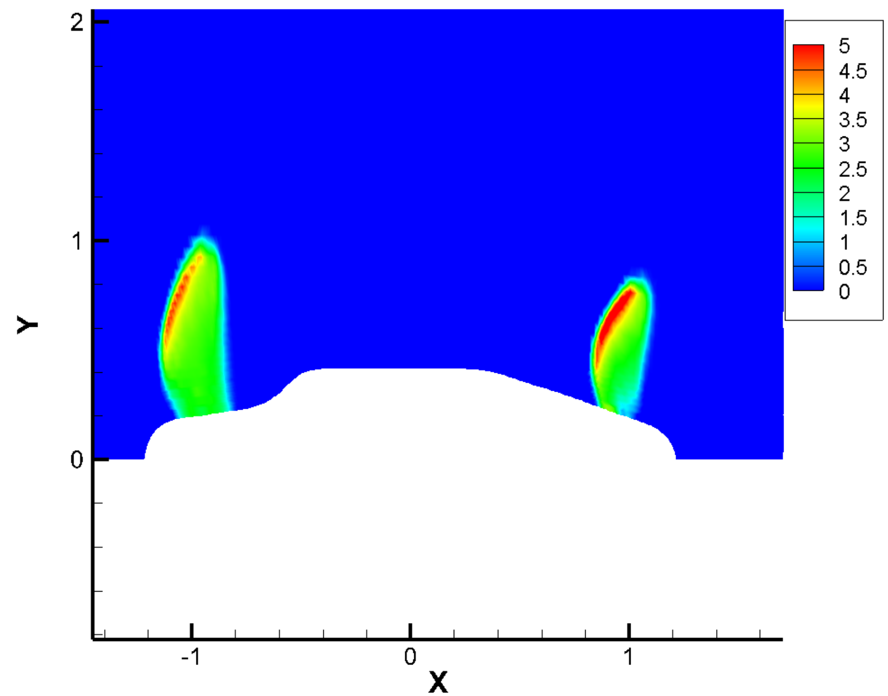

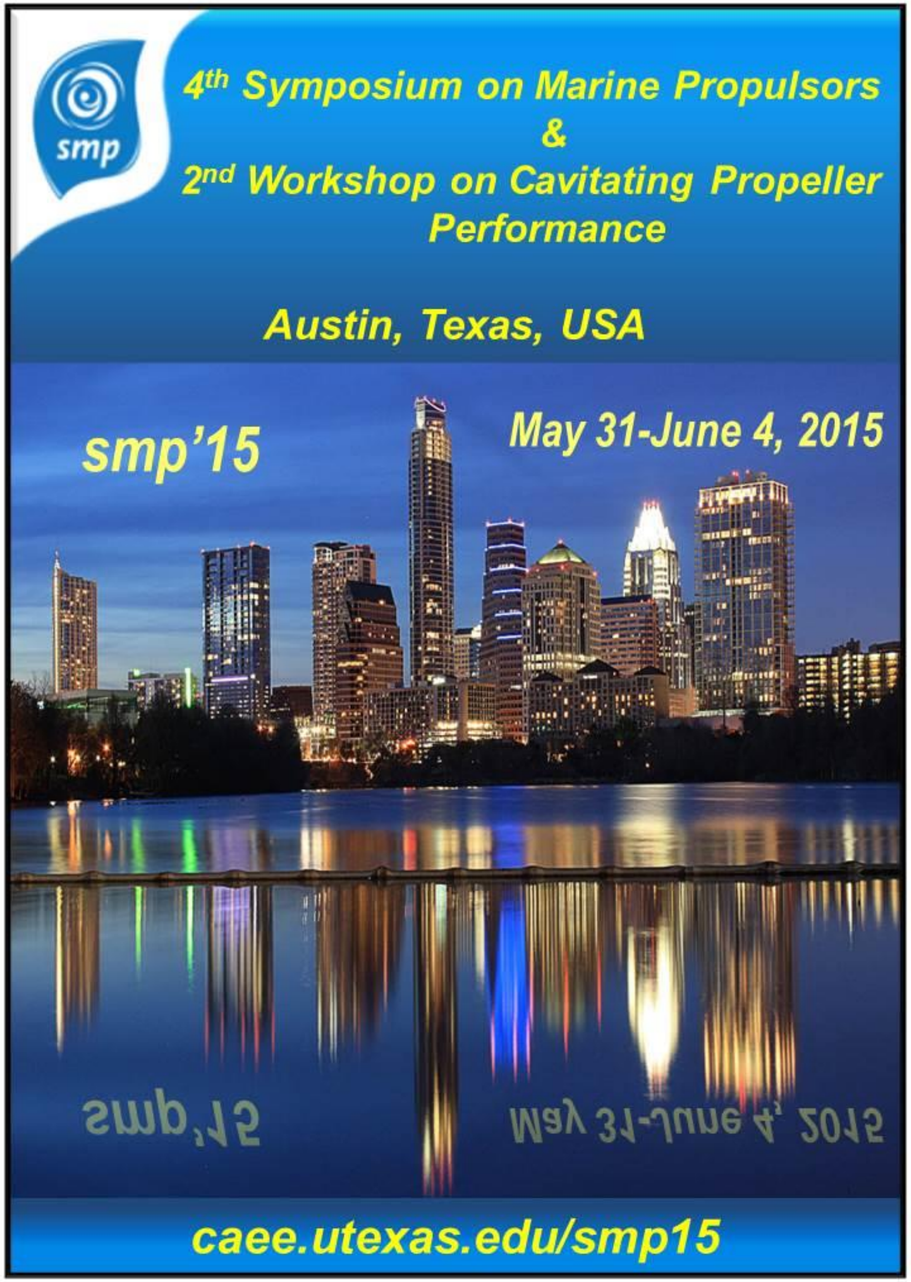

For most recent developments on Marine Propulsors